SSCL-N-734

THERMAL CONDUCTIVITY OF A POLYMIDE FILM BETWEEN 4.2 AND 300K, WITH AND WITHOUT ALUMINA PARTICLES AS FILLER*

D. L. Rule, D. R. Smith and L. L. Sparks
National Institute of Standards and Technology
Chemical Engineering Science Division
Boulder, CO 80303

for the

Superconducting Super Collider Laboratory†
2550 Beckleymeade Ave.
Dallas, TX 75237

August 1990

*This work was supported by the National Institute of Standards and Technology under SSC Laboratory P.O. # 455510, for the U.S. Department of Energy.

†Operated by the Universities Research Association, Inc., for the U.S. Department of Energy under Contract No. DE-AC02-89ER40486.

TABLE OF CONTENTS

LIST OF TABLES

LIST OF FIGURES

ABSTRACT

INTRODUCTION

RELEVANT PREVIOUS WORK

DESCRIPTION OF APPARATUS

DESCRIPTION OF SPECIMENS
- Construction
- Measurement of Surface Roughness

EXPERIMENTAL PROCEDURE
- Cutting PPMI Film
- Building a Specimen
- Mounting a Specimen in the Apparatus
- Experimental Conditions

COMPUTATION OF THERMAL CONDUCTIVITY

THERMAL CONDUCTIVITY OF PPMI FILM
- Representation of Data
- Dependence of Thermal Conductivity on Temperature
- Reproducibility of Tests
- Dependence of Conductivity on Film Thickness
- Effect of Thermal Contact Resistance
- Dependence of Conductivity on Applied Pressure
- Effect of Heat Treatment on Conductivity

COMPARISON WITH RESULTS FROM OTHER STUDIES

SUMMARY

ACKNOWLEDGMENTS

REFERENCES

APPENDIX

LIST OF TABLES

Table 1. Specimen identification.

Table 2. Physical characteristics of the specimens.

Table 3. Coefficients of $\lambda(T)$ for five PPMI film specimens.

Table 4. Location index for remaining data tables and figures for all PPMI film specimens.

Table 5. Experimental conductivity as a function of temperature for PPMI film H-003.

Table 6. Experimental conductivity as a function of temperature for PPMI film H-003-R (retest).

Table 7. Thermal conductivity calculated for selected temperatures, from eq (1), for specimen PPMI film H-003.

Table 8. Experimental conductivity as a function of temperature for PPMI film HN-003.

Table 9. Thermal conductivity calculated for selected temperatures, from eq (1), for specimen PPMI film HN-003.

Table 10. Experimental conductivity as a function of temperature for PPMI film MTL-003.

Table 11. Thermal conductivity calculated for selected temperatures, from eq (1), for specimen PPMI film MTL-003.

Table 12. Experimental conductivity as a function of temperature for PPMI film MT-003.

Table 13. Experimental conductivity as a function of temperature for PPMI film MT-003-R (retest).

Table 14. Thermal conductivity calculated for selected temperatures, from eq (1), for specimen PPMI film MT-003.

Table 15. Experimental conductivity as a function of temperature for PPMI film MT-001.

Table 16. Thermal conductivity calculated for selected temperatures, from eq (1), for specimen PPMI film MT-001.

Table 17. Experimental conductivity and $\Delta T/Q$ per layer of film as a function of applied mechanical pressure.

Table 18. Experimental conductivity as a function of temperature for PPMI film HN-Heat.

LIST OF FIGURES

Figure 1. Specimen chamber for thermal-conductivity probe.

Figure 2. Cutting of PPMI film.

Figure 3. Construction of a PPMI specimen.

Figure 4. Measuring the size of the specimen stack.

Figure 5. Thermal conductivity of PPMI film specimens H-003 and H-003-R, (repeated measurements on same specimen), plotted on linear scales to clarify the high-temperature behavior.

Figure 6. A re-plot of data in fig. 5 on logarithmic scales, clarifying the low-temperature behavior.

Figure 7. Relative deviations of experimental data from calculated thermal conductivity for PPMI film specimens H-003 and H-003-R.

Figure 8. Thermal conductivity of PPMI film specimen HN-003, plotted on linear scales to clarify the high-temperature behavior.

Figure 9. A re-plot of data in fig. 8 on logarithmic scales, clarifying the low-temperature behavior.

Figure 10. Relative deviations of experimental data from calculated thermal conductivity for PPMI film specimen HN-003.

Figure 11. Thermal conductivity of PPMI film specimen MTL-003, plotted on linear scales to clarify the high-temperature behavior.

Figure 12. A re-plot of data in fig. 11 on logarithmic scales, clarifying the low-temperature behavior.

Figure 13. Relative deviations of experimental data from calculated thermal conductivity for PPMI film specimen MTL-003.

Figure 14. Thermal conductivity of PPMI film specimens MT-003 and MT-003-R (repeated measurements on same specimen), plotted on linear scales to clarify the high-temperature behavior.

Figure 15. A re-plot of data in fig. 14 on logarithmic scales, clarifying the low-temperature behavior.

Figure 16. Relative deviations of experimental data of fig. 14 from calculated thermal conductivity.

Figure 17. Thermal conductivity of PPMI film specimen MT-001, plotted on linear scales to clarify the high-temperature behavior.

Figure 18. A re-plot of data in fig. 17 on logarithmic scales, clarifying the low-temperature behavior.

Figure 19. Relative deviations of experimental data from calculated thermal conductivity for PPMI film specimen MT-001.

Figure 20. Thermal conductivity of four PPMI film specimens composed of 76 μm film, plotted on linear scales to clarify the high-temperature behavior.

Figure 21. A re-plot of data in fig. 20 on logarithmic scales, clarifying the low-temperature behavior.

Figure 22. Intercomparison of thermal conductivity of PPMI film specimens MT-003 and MT-001.

Figure 23. Intercomparison of relative deviation of experimental data for PPMI film specimen MT-001 with calculated thermal conductivity and experimental data for film specimen MT-003.

Figure 24. Thermal contact resistance, ΔT/Q, per layer of PPMI film, at a mean specimen temperature of 277.5 K, as a function of presence or absence of grease on the interfaces, and of number of interfacial contacts.

Figure 25. Thermal contact resistance, ΔT/Q, per 76 μm layer of PPMI film, as a function of applied pressure, for mean specimen temperatures of 277.8 K, 80.3 K, and 8.3 K.

Figure 26. Thermal conductivity as a function of applied pressure, corresponding to the data for thermal contact resistance shown in fig. 25.

Figure 27. Effect of heat treatment on the thermal conductivity of PPMI film.

Figure 28. Relative deviations of data of fig. 27 from calculated thermal conductivity.

Figure 29. Thermal conductivity of PPMI film specimens composed of layers of film 76 μm thick, as in fig. 21. Conductivity data for Kapton or other polyimide films (Vespel, Kerimid, polyethylene, and Mylar) are also given for intercomparison.

Figure A1. **(Lower)**: Image, from a scanning tunnelling microscope (STM), of a single film of type H unfilled (neat) PPMI.
(Upper): A surface roughness profile along the path marked on the lower STM image.

Figure A2. **(Lower)**: STM image of type HN unfilled (neat) PPMI film.
(Upper): A surface roughness profile for a scan across the surface.

Figure A3. **(Lower)**: STM images of type MTL alumina-filled PPMI film.
(Upper): A surface roughness profile for a scan across the surface.

Figure A4. **(Lower)**: STM images of type MT alumina-filled PPMI film.
(Upper): A surface roughness profile for a scan across the surface.

Figure A5. **(Lower)**: STM images of type MT alumina-filled PPMI film.
(Upper): A surface roughness profile for a scan across the surface.

THERMAL CONDUCTIVITY OF A POLYIMIDE FILM BETWEEN 4.2 AND 300 K, WITH AND WITHOUT ALUMINA PARTICLES AS FILLER

D. L. Rule, D. R. Smith, L. L. Sparks

National Institute of Standards and Technology
Chemical Engineering Science Division
Boulder, Colorado 80303

ABSTRACT

The thermal conductivity of several types of a commercial polyimide (specifically, polypyromellitimide: PPMI) film was measured over a range of temperatures from 4.2 to 300 K using an unguarded steady-state parallel-plate apparatus. Specimens were made by stacking multiple layers of film together. Conductive grease was used between layers of film to reduce thermal contact resistance. Two specimens were made from two different types of neat (unadmixed) film with a thickness of 76 μm, and three specimens were made from films containing two different amounts of admixed alumina filler and having thicknesses of 25 μm or 76 μm. The conductivity of PPMI film increases with the amount of alumina filler present. The thermal conductivity of specimens made from film of the same type but of different thickness is independent of film thickness, within the limits of experimental uncertainty. The thermal conductivity of a specimen subjected to a simulated curing process by being held at a temperature of 150°C for ninety minutes was indistinguishable from that of a similar, control specimen not subjected to such treatment.

INTRODUCTION

The thermal conductivity of many polymeric materials, including polypyromellitimide (PPMI) in particular, is not well known over ranges of temperature where such polymers already find wide application. PPMI film has several desirable properties; among these are good tensile strength and mechanical toughness. As a polymeric material, however, PPMI has a thermal conductivity which is relatively low compared to that of some other cryogenic insulating materials. This reduced conductivity makes PPMI film a candidate for applications such as electrical insulation between electrical windings at low temperatures for superconducting magnets. We report measurements of thermal conductivity for two different thicknesses of PPMI film, either neat (unadmixed), or filled with powdered alumina. PPMI film is commonly known as Kapton*.

---

* Kapton is a registered trademark for a proprietary PPMI film. Vespel and Kerimid are trademarks for polyimide resins used for castings or moldings. These particular PPMI products, as well as other products named

Glassy or otherwise disordered materials such as epoxy or polymeric plastics strongly scatter phonons at all temperatures. The effect of powdered filler material within a surrounding matrix is to increase the thermal resistance of the composite by enhancing the scattering of the phonons carrying the thermal energy. This effect is accentuated if the velocities of sound in the two media and their densities are very different. For composites of epoxy that contain fillers, the thermal conductivity of the composite can be either greater or less than that of the epoxy matrix, depending on the size and kind of the particles used as the filler[1,2,3]. For example, fine particles of dielectric material within an epoxy or polymeric matrix will increase phonon scattering and result in a material that is a poorer thermal conductor (better thermal insulator). The scattering of phonons is enhanced for fillers having smaller grain size. The conductivity of composites of epoxy and nonmetallic filler particles at temperatures below 10 K is much lower than would be expected on the basis of high-temperature behavior, and the difference is greater, the lower the temperature[1].

On the other hand, a filler of metallic or other highly conductive powder at high filling factor can be used to increase the thermal conductivity of a dielectric matrix, by shunting the flow of heat through the grains of conductive powder and bypassing the poorly conducting path through the matrix, but at temperatures below 10 K the small size of the particles may still increase phonon scattering and cause a net increase in thermal resistance.

RELEVANT PREVIOUS WORK

Literature surveyed in conjunction with the current experimental study revealed some previous work concerning the thermal conductivity of films of PPMI or similar polymers. The experimental techniques used, and the data obtained in these studies are pertinent to evaluating our data. The discussion below briefly summarizes previous experimental results thought to be relevant to this work.

For analyzing the thermal conductivity of epoxy resin matrix containing powdered glass, quartz, alumina, or diamond, Meredith and Tobias[4] extended a basic formula of Rayleigh[5] to the regime of higher volume concentrations of filler. Garrett and Rosenberg[1] found this approach to be a satisfactory basis for analyzing experimentally obtained conductivity values, assuming the filler particles to be spheres. The concentration and conductivity of the filler particles must both be known.

In the course of an investigation of thermal grounding of copper electrical leads bonded to polyimide film, Radebaugh, Frederick, and Siegwarth[6] measured the thermal conductivity of Kapton at temperatures from 0.1 to 4.2

---

in this report (Mylar, OMEGA, Apiezon grease) are identified only to specify the material used in this and in other studies cited as background; endorsement of these products or their manufacturers by NIST or by the U.S. government is neither intended nor implied.

K. The leads were of copper foil 36 μm thick, and the polyimide film was 76 μm thick. The foil was bonded to one side of the polyimide film with thin sheets of thermoplastic polyester resin cured at 150°C, which thus exposed the polyimide film to the same curing temperature. The thermal conductivity of the polyimide film was found to be about 5 mW/(m·K) at 4.2 K.

Vespel polyimide resin is an amorphous, cast, solid form of PPMI. Locatelli, Arnaud, and Routin[7] measured the thermal conductivity of three different types (neat, filled with graphite, or filled with fibrous glass) of this resin over the range of temperature from 0.08 to about 2 K. The specimens were cylinders 5 mm in diameter and 50 mm long. Over this range of temperature the resin exhibited a linear dependence of the logarithm of thermal conductivity on the logarithm of temperature. It is risky, but possibly informative, to assume that their conductivity-temperature relation may be safely extrapolated to temperatures somewhat higher (4.2 K) than their upper limit of measurement (2 K). When such an extrapolation is performed (graphically) to estimate the thermal conductivity, a value of about 10 mW/(m·K) is found for the conductivity of neat Vespel SP 1 resin at 4.2 K. Details of the experimental technique used to measure the thermal conductivity were not given in the paper by Locatelli, et al.

Kerimid is another amorphous, solid form of PPMI. Claudet, Disdier, and Locatelli[8], using the "double flux" method[9], measured the thermal conductivity of Kerimid resin, in combination with two different types of powdered alumina filler. The two types were A_1: hexagonal, particle size, 1.5 μm; and A_2: cubic particle size, 0.02 μm. These workers also found a linear dependence between the logarithm of the thermal conductivity and logarithm of the temperature. They found the conductivity of neat resin to be 38 mW/(m·K) at 4.2 K. Admixture to the resin of 56 mass percent of A_1 alumina as filler reduced the conductivity at 4.2 K to 15.5 mW/(m·K). This was a reduction of conductivity by a factor of about 2.5 in comparison to the value for neat resin. Increasing the concentration of this same alumina filler to 65 mass percent gave a conductivity of about the same value, 14 mW/(m·K). They felt these results were in good agreement with a value (11 mW/(m·K) they cite from an earlier study by Van de Voorde[10] on neat Vespel SP4 resin. Their use of A_2 alumina as filler (57 percent by mass) reduced the conductivity at 4.2 K by a factor of 10 to 3.9 mW/(m·K) in comparison to the value for neat resin. Use of 65 percent by mass of A_2 alumina as filler reduced the conductivity at 4.2 K to 1.7 mW/(m·K), a reduction by a factor of 22. They attribute the much lower values for the specimens of resin filled with A_2 alumina to the presence of some porosity, as suggested by appreciable differences between calculated and measured densities.

Muller[11] measured the thermal conductivity of several kinds of plastic tapes (polysulfone, polyethylene, polycarbonate, polypropylene with urethane binder, and polypropylene with polyethylene binder). Such tapes were being considered for insulation of cryogenic power cables. He used a modified steady-state technique that established a temperature gradient between two copper plates separated by four layers of polymeric film. Measurements were performed with the tapes in vacuum and in helium gas at pressures from 0 to 710 kPa (0 to 100 psi). No mention was made of use of any material between the layers of film to reduce thermal contact resistance. Muller found the

thermal conductivity to depend on gas pressure for values between 0 and 170 kPa (25 psi). Above these pressures the conductivities of the polyethylene and polycarbonate films were independent of gas pressure. The thermal conductivities of these films at 6 K ranged from 6 to 9.2 mW/(m·K).

Wipf[12] measured thermal resistances of copper surfaces separated by films of Kapton, Mylar (polyethylene terephthalate) or mica, over the range of temperature from 4 to 30 K. He used a stack of an alternating series of insulating film and 1-mm copper blocks in an unguarded apparatus. By assuming that the thermal conductivity of the bulk material does not depend on contact pressure, but that the contact resistance (and its reciprocal, the interfacial contact conductance) does, he found that the effective interfacial conductance saturates, or becomes constant, at high pressure (above about 100 MPa). At low temperatures an approximately linear dependence of the logarithm of thermal conductivity of Kapton film on the logarithm of temperature was observed. At 5 K the conductivity of the film was 10 ± 2 mW/(m·K) and at 10 K its conductivity was approximately 20 mW/(m·K). Wipf concluded that at low temperatures polyimide film is, among solids, "one of the worst"[10] thermal conductors (best thermal insulators). The conductivity depended strongly on contact pressure between the contacting copper surfaces and the film specimens, implying poor thermal contact below approximately 100 MPa.

Choy, Leung, and Ng[13] used laser-flash diffusivity to measure the thermal diffusivity of films of polycarbonate, polyvinylidene fluoride, polyimide, and polyethylene terephthalate. Combining the experimental diffusivity data with specific heat data obtained from the literature, they then calculated the thermal conductivity. At 298 K, the thermal conductivity of the polyimide film (Kapton Type H), for thicknesses of 14, 26, 51 and 130 μm, was 166 ± 4 mW/(m·K).

One technique for determining thermal conductivity is to use the relation between temperature rise and time for a copper block of known heat capacity, heated through a thin film of specimen interposed between the block and the source of heat. Using such a method, called a "thick-film integrator", together with a laser-flash thermal diffusivity apparatus, Witek, Guerrero, and Onn[14] determined the thermal conductivity at room temperature of polyimide film (Kapton 100 H-N) matrix filled with powdered alumina. The size of the alumina filler particles was not given. The thermal conductivity determined by the thick-film integrator at room temperature varied approximately linearly from 100 mW/(m·K), at 0 volume percent (neat polyimide) of alumina filler, to about 380 mW/(m·K), at 45 volume percent of filler.

Lambert[15] quoted manufacturer's values for the thermal conductivity of Kapton H polyimide film. The conductivity values given varied from about 160 mW/(m·K) at 25°C to 178 mW/(m·K) at 200°C.

Steere[16] established that a specimen of polymeric material may be built up of a stack of thin films without adversely affecting the accuracy of measurement of thermal conductivity. He used films of polyethylene terephthalate (PET; type-A Mylar) with a thickness of 25 μm (0.001 in) alternating with ultra-thin (2.5 μm) foils of constantan. No grease or other thermal

contact medium was used between the foils. The conductivity was measured by a transient technique while the stack of films was held in an ordinary bench vise. The compressive force used was not quantified, but was described as "no[t] excessive". His values for the thermal conductivity of this PET film varied from about 130 to 140 mW/(m·K) at temperatures from 210 to 270 K.

Hust and Boscardin[17] measured the thermal conductivity of aluminum disks 0.25 mm (0.01 in) thick coated on both sides with polyester-amide-imide film (OMEGA). The mean specimen temperatures ranged from 4 to 300 K. A stack of 63 of these disks was built up with Apiezon N grease on both surfaces of each disk. The total thickness of the grease during the measurement was negligible, and no increase in thermal resistance was expected. At low temperatures a linear dependence of the logarithms of thermal conductivity and temperature was observed. The slope of the functional relation began decreasing at temperatures above 100 K and was almost flat at 300 K. The values of conductivity found for this particular film were about 24 mW/(m·K) at 4 K, about 140 mW/(m·K) at 78 K, and about 200 mW/(m·K) at 300 K.

Lee[18] used a dynamic measurement technique to measure the thermal conductivity at room temperature of thin films of polyterephthalate (PET; Mylar) in single thicknesses of 76 and 127 μm, and in combined thicknesses of 203 and 254 μm; polymethylmethacrylate (PMMA), in six thicknesses ranging from 12 to 80 μm; and polystyrene (PS), in six thicknesses ranging from 12 to 150 μm. To improve thermal contact at the interfaces, the surfaces of the polymer films were wet with a small amount of mineral oil and the measuring stack of isothermal blocks and polymer film was loaded with weights of 207 or 300 g. Some residual contact resistance was still observed and was measurable with the technique used. The observed thermal conductivities at room temperature were: PS, 169 mW/(m·K); PMMA, 201 mW/(m·K); and PET, 189 mW/(m·K).

DESCRIPTION OF APPARATUS

The apparatus used here to measure thermal conductivity is a modified, unguarded, "fixed-point" apparatus[19] based on a method of axial one-dimensional heat flow. The specimen chamber is shown schematically in figure 1. A specimen of known length and cross-sectional area is compressed between two isothermal copper blocks.

Three stainless-steel bolts clamp the specimen between the two isothermal copper blocks. The upper limit of clamping pressure attainable with these bolts is estimated as about 17 MPa for specimens having a diameter of 19 mm (0.75 in). This maximum pressure is determined by the total force bearable by the three clamping bolts, and is greater for specimens of smaller diameter. However, the use of a specimen of smaller diameter would lead to a smaller flow of heat through the specimen, a greater fraction of heat through the clamping bolts, and a greater uncertainty in the quantity of heat flowing through the specimen. The flow of heat bypassing the specimen through the

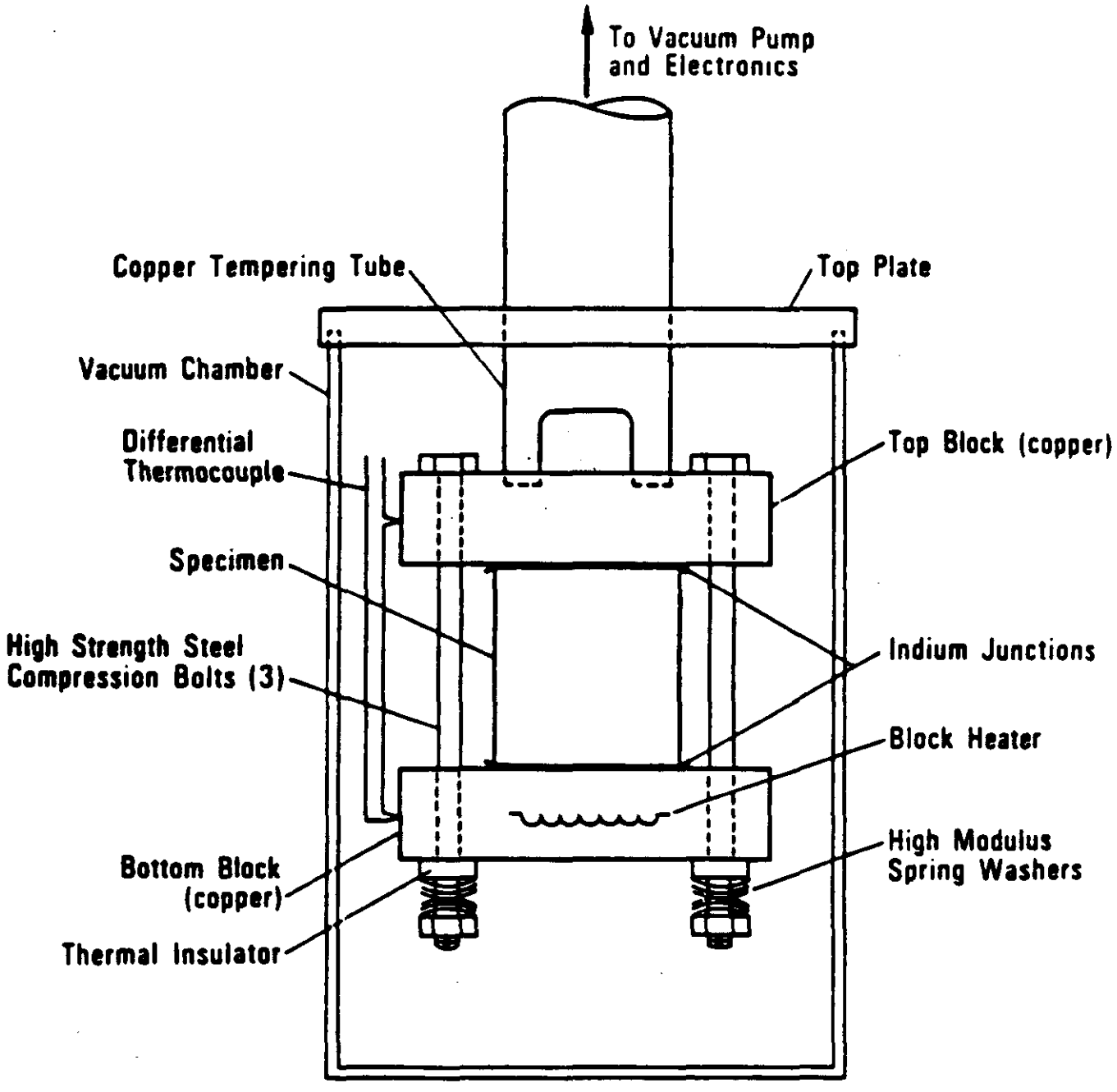

Figure 1. Specimen chamber for fixed-point compression probe.

bolts is known from previous calibration runs, and is subtracted from the total heat produced in the heated isothermal block to obtain the quantity of heat passing through the specimen.

The upper isothermal block is thermally anchored by conduction through a copper tempering tube to the top of the specimen chamber, which is immersed in one of four constant-temperature (fixed-point) baths. This upper block maintains the cold-side temperature of the specimen. The nominal temperatures of these fixed-point baths are: 4 K (determined by a bath of liquid helium), 76 K (liquid nitrogen), 194 K (a mixture of dry ice and alcohol), or 273 K (a mixture of pure ice and water).

The temperature of the lower block is maintained by controlling the electric power supplied to its attached heater; this determines the hot-side temperature of the specimen as well as fixing the temperature difference across the specimen. The total power supplied to the hot block is determined from measurements of the voltage and current to its resistive heating element. The heat flowing through the specimen is computed by subtracting the calibrated heat flow through the compression bolts from the total power. Approximately 60% of the total power passes through the specimen.

A AuFe-NiCr thermocouple measures the cold-block temperature, and a differential thermocouple of the same alloys measures the difference in temperature between the hot and cold blocks. The temperature differences established between the blocks are typically 1, 2, 4,..., and 64 K, differing by factors of 2. These temperature differences permit the use of different mean temperatures within the specimen subject to the constraint of the fixed cold-side temperatures.

DESCRIPTION OF SPECIMENS

Construction

Specimens were made by stacking together multiple layers of PPMI film of the same type. Some of the tested films contained particles of alumina as a filler to increase the conductivity; the size and amount of these alumina particles in the film were not available from the manufacturer. Table 1 provides the specimen identification. The thickness of the films used to construct most of the specimens was nominally 76 μm (0.003 in), but one specimen was made with nominally 25 μm (0.001 in) film. Table 2 lists the diameter and total thickness of each specimen stack, as well as the total number of film layers each stack contained, from which the thickness per layer was computed. The agreement of the measured thickness per layer of an actual built-up specimen (25 μm or 76 μm) with the nominal thickness (26 μm; 73 to 79 μm) is good, within experimental imprecision. The arithmetic mean of the measured thickness of the nominally 76.2 μm thick film used in the first seven specimens is 76.5 μm.

Table 1. Specimen identification.

Specimen	Lot Number	Nominal Film Thickness (μm)	(in)	Material
H-003	247-3	76	0.003	Unfilled film
H-003-R	247-3	76	0.003	Retest of film H-003
HN-003	256-A	76	0.003	Unfilled film
HN-heat	256-A	76	0.003	Retest of spec. HN-003 after heat treatment
MTL-003	327-B	76	0.003	Low alumina content
MT-003	Roll	76	0.003	High alumina content
MT-003-R	303	76	0.003	Second specimen, MT-003
MT-003-P		76	0.003	Third specimen, MT-003
MT-001	332-B	25	0.001	High alumina content

Table 2. Physical characteristics of the specimens.

Specimen	Diameter (mm) ?	Thickness (mm) ?	Number of Layers	Thickness per Layer (μm) ?	Surface Roughness (nm)** ?
H-003	19.45	2.54	33	77	67
H-003-R	19.43	2.60	33	79	
HN-003	19.43	2.47	33	75	32
HN-Heat	19.43	2.46	33	75	
MTL-003	19.43	3.71	51	73	250
MT-003	19.45	6.44	84	77	390
MT-003-R	19.43	6.53	84	78	
MT-003-P	19.43	6.38	84	77	
MT-001	19.43	6.61	252	26	390

** Measurements of surface roughness of filled films revealed the existence of some localized peaks. Specimen MTL-003 had some peaks with heights of up to 1000 nm, and MT-003 had 750 nm peaks. The MT-001 film also had some peaks, of undetermined size.

Measurement of Surface Roughness

Information on the surface roughness of the PPMI films was also not available from the manufacturer. A colleague at NIST measured the surface roughness of several film specimens with a scanning tunneling microscope (STM). A 30 nm layer of gold was evaporatively deposited on each clean film surface. This is the usual procedure for providing a conductive surface to be imaged; the gold layer is too thin to obscure details of surface roughness on the scale of importance here. The STM uses feedback circuitry on the tunneling current between a conductive specimen and a atomically sharp needle to map the surface topography. A portion of the surface of the specimen was imaged and then a cross section of that image was used to determine the surface roughness. The resulting images and surface-roughness scans for five different film specimens are given in the Appendix. STM scans of the film surface indicate that the unfilled films have a much smoother surface than the filled films (table 2). Surface scans and images of MT and MTL films exhibited some localized peaks which may correspond to grains of alumina protruding from the surface of the film.

EXPERIMENTAL PROCEDURE

Cutting PPMI Film

For several technical reasons, the fixed-point thermal conductivity apparatus requires a specimen with a uniform cross-sectional area and a length of 6 to 18 mm. Thus, to be suitable for mounting in this apparatus a specimen of PPMI film has to be made as a stack of individual layers of film (circular disks). The disks of film must be cut with a very clean outside edge so that they can be stacked together without interference from the cut edges. After trying several methods of cutting disks, we found a common laboratory circular gasket cutter to be most suitable for cutting single disks of film. In the cutting operation the film was sandwiched between sheets of paper. Use of a thick backing sheet of Teflon prolonged the life of the cutting edge of the cutter. The individual disks so produced were very uniform in size. Figure 2 shows the cutter, film and backing sheet.

Building a Specimen

In order to determine the intrinsic thermal conductivity of the film in the specimen stack, we developed special procedures for constructing and mounting a specimen to minimize thermal contact resistance between layers of film. Adhesives, having intrinsically high viscosity, could not be used between the layers of film to reduce contact resistance without introducing non-negligible amounts of material different from the film to be tested. Instead, a specimen stack was constructed by applying thermally conductive grease to the contact surfaces of each film disk when compressing the disks together.

Figure 2. A single layer of PPMI film was sandwiched between paper and cut with a circular gasket cutter. Use of a backing sheet of PTFE prolonged the life of the cutting edge.

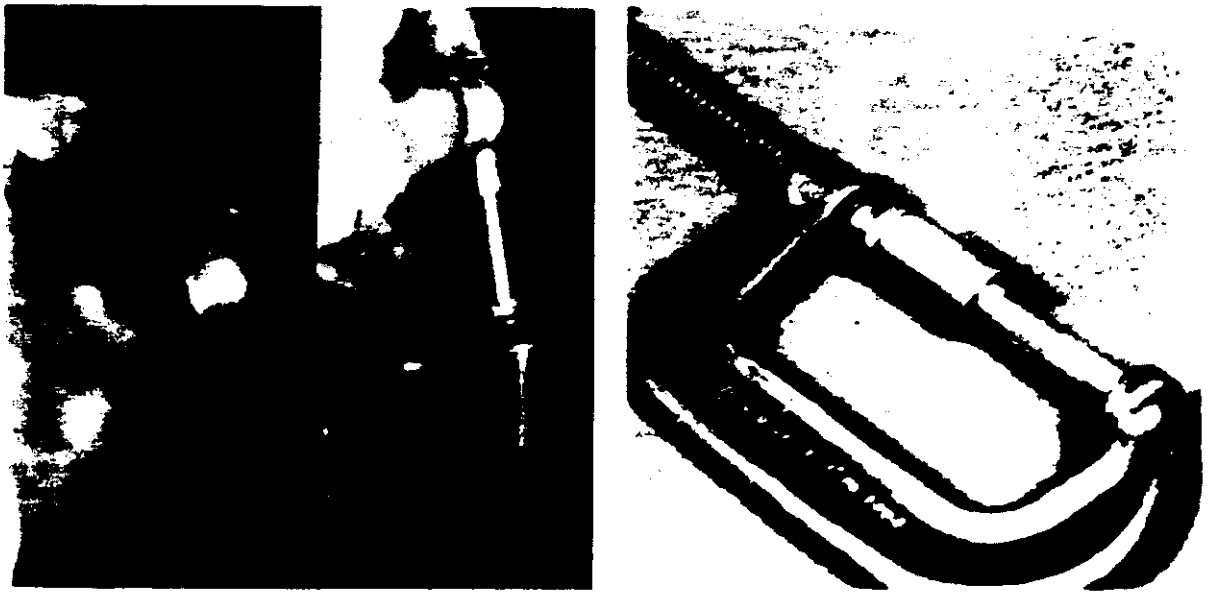

Figure 3. Building a PPMI specimen involved: (a) stacking the greased disks of film in a restraining tube and then (b) compressing the layers between two copper blocks with a C-clamp. Excess grease was removed by wiping with a paper towel (no solvent was used).

The grease used here was chosen for the following considerations: (a) low viscosity, permitting it to flow out readily from between neighboring disks and thereby reduce contact resistance without contributing its own thermal resistance; (b) absence of thermally conductive filler, which, while increasing thermal conductivity would also adversely affect the viscosity; (c) low glass transition temperature, giving it favorable mechanical properties in the stack during cool-down; (d) relatively high thermal conductivity; and (e) solubility in common solvents, permitting it to be easily cleaned from the apparatus after the specimen was removed.

To construct a specimen, we mounted disks of PPMI film within a restraining tube which maintained the alignment of the disks as they were pressed together between two copper blocks with a C-clamp (fig. 3). While the specimen stack was compressed, the diameter and length were measured (fig. 4) with an imprecision of 13 μm (0.0005 in). After the stack of disks was compressed, the tube was removed from around the film disks and excess grease was wiped away with dry cotton swabs or clean paper towel (no solvent was used). The specimen was then removed from the C-clamp and mounted into the apparatus.

With only a few exceptions which will be explicitly identified, the use of grease as described here was the normal procedure followed in constructing all specimens from layers of film.

Mounting a Specimen in the Apparatus

To mount a specimen in the conductivity apparatus, we first centered it between the two isothermal copper blocks. Contact between the blocks and the specimen was effected by tightening the three compression bolts with a calibrated torque wrench to 1.6 N·m (14 in·lb) of torque. This same value of torque was used in all experiments. By this means a clamping pressure of approximately 17 MPa (2.4 kpsi) was applied to the specimen (at room temperature) in an effort to minimize the effect of thermal contact resistance. Higher values of torque were not used because this value was believed to be approaching that at which plastic deformation of the threads on the compression bolts would begin. The change in clamping pressure due to cooling the specimen to cryogenic temperatures, while not accurately known, is believed to be relatively small and not seriously to affect the measurements of conductivity reported here. After the specimen was compressed in the apparatus any additional excess grease was removed.

Experimental Conditions

Steady-state measurements were made with the specimens in a vacuum environment of 1.07×10^{-2} Pa (8×10^{-5} Torr). With the specimen chamber in one of the fixed-point baths described earlier, mean specimen temperatures could be chosen in the range from 4.2 to 300 K. In each case (with one exception described later), specimens had the conductive grease applied to all contact surfaces.

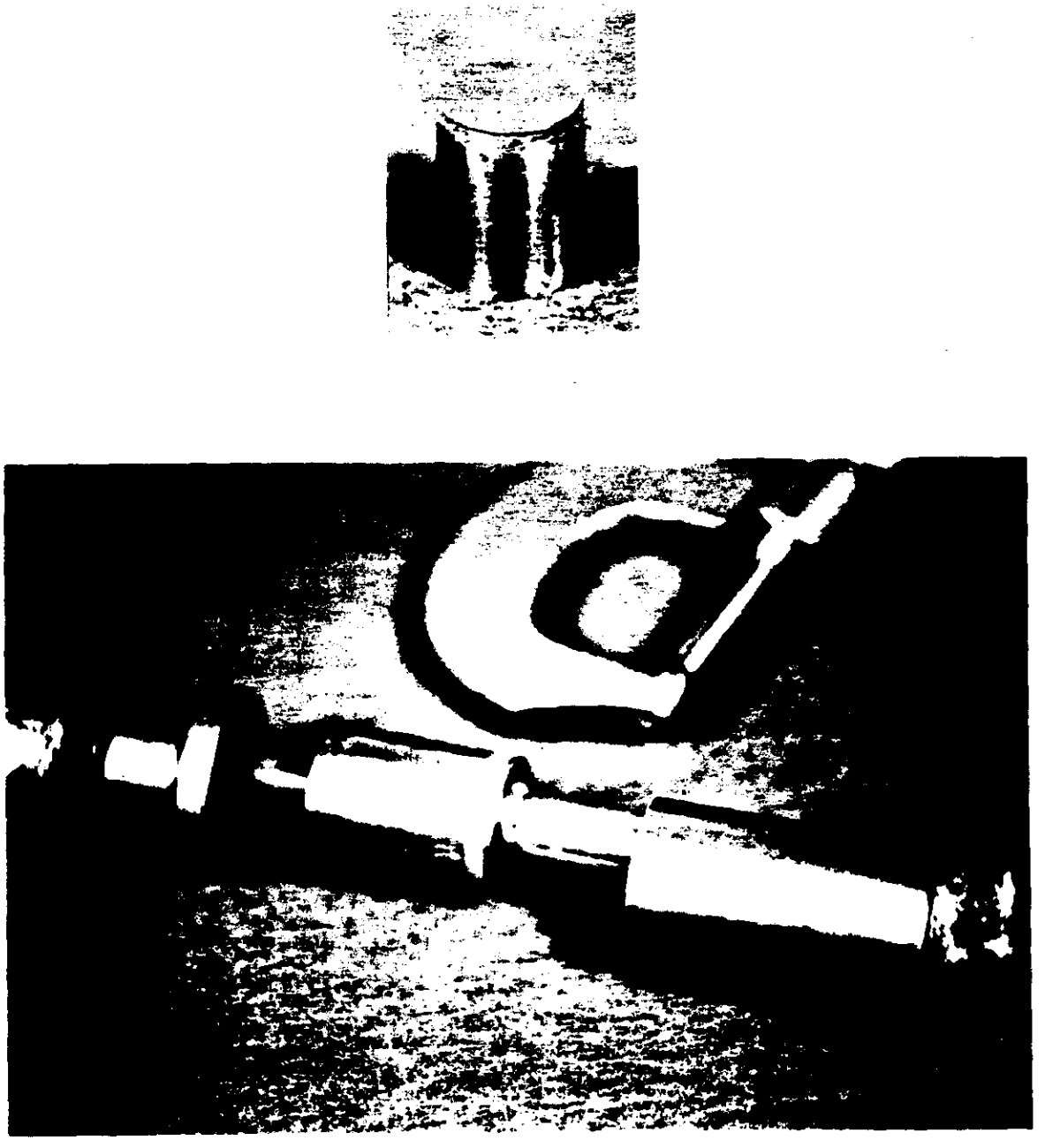

Figure 4. Diameter and length of the specimen stack were measured while the stack was compressed in the C-clamp.

COMPUTATION OF THERMAL CONDUCTIVITY

Knowledge of the power, Q_{spec}, through the specimen, specimen geometry (thickness, ℓ and cross-sectional area, A) and temperature difference, ΔT, across the specimen allow the mean thermal conductivity, λ, to be calculated. The calculation is performed using the one-dimensional approximation of Fourier's law,

$$Q_{spec} = \lambda \cdot A \cdot (dT/dx), \qquad (1)$$

recast into the approximate form

$$\lambda = (Q_{spec}/A)/(\Delta T/\ell). \qquad (2)$$

Here the ratio $\Delta T/\ell$ in eq (2) approximates the derivative dT/dx in eq (1), and the conductivity obtained is the value averaged over the range of temperature defined by the temperature difference ΔT across the specimen.

When the thermal conductivity depends nonlinearly on temperature, as it does for these specimens, the large values of temperature difference used during these measurements can introduce bias in the values of thermal conductivity calculated from eq (2). This is due to curvature of the conductivity function over the range of temperature ΔT. These biases were removed during analysis of the thermal conductivity data by use of an integral technique[20] which gives the correct functional dependence for the thermal conductivity with temperature. As is conventional, all conductivity data in the figures are plotted as a function of the (arithmetic) mean temperature of the specimen.

THERMAL CONDUCTIVITY OF PPMI FILM

Representation of Data

The function chosen to fit the thermal conductivity data as a function of temperature for each specimen was of the form

$$\lambda(T) = \sum_{i=1}^{n} a_i \; [\ell n \; (T+1)]^i, \qquad (1)$$

where n = 4. The resulting values of a_i for each specimen are listed in table 3.

Table 3. Coefficients of $\lambda(T)$.

Spec.	a_1	a_2	a_3	a_4
H-003	$15.549\ 709 \times 10^{-3}$	$-17.417\ 525 \times 10^{-3}$	$82.690\ 158 \times 10^{-4}$	$-81.952\ 869 \times 10^{-5}$
HN-003	$30.782\ 762 \times 10^{-3}$	$-32.061\ 706 \times 10^{-3}$	$12.444\ 129 \times 10^{-3}$	$-10.070\ 564 \times 10^{-4}$
MTL-003	$35.506\ 858 \times 10^{-3}$	$-39.018\ 329 \times 10^{-3}$	$15.500\ 030 \times 10^{-3}$	$-13.132\ 755 \times 10^{-4}$
MT-003	$43.345\ 123 \times 10^{-3}$	$-50.529\ 112 \times 10^{-3}$	$19.656\ 630 \times 10^{-3}$	$-16.480\ 966 \times 10^{-4}$
MT-001	$48.310\ 057 \times 10^{-3}$	$-53.541\ 715 \times 10^{-3}$	$20.399\ 570 \times 10^{-3}$	$-17.040\ 603 \times 10^{-4}$

The following format is used to present the thermal conductivity data for each of the film specimens (made from films H-003, HN-003, MTL-003, MT-003, or MT-001), in a sequence composed typically of five figures and tables:

First, the experimental conductivity data obtained at each mean specimen temperature are tabulated (additional data are listed separately if the specimen was remeasured).

Second, smoothed values of conductivity calculated from the fitted curve (using applicable coefficients) are listed in a following table, with values of mean specimen temperature differing by 0.1 K, for mean temperatures from 4.1 to 10 K; with mean temperature values differing by 1 K, for temperatures from 10 to 100 K; and then with values differing by 10 K for temperatures from 100 to 300 K.

Third, the conductivity data are plotted with linear scales of conductivity and temperature, to clarify behavior in the high-temperature (200 to 300 K) regime.

Fourth, the data are also presented with logarithmic scales along the conductivity and temperature axes, to clarify the behavior in the low-temperature (4 to 200 K) regime.

Last, a plot of the relative (percent) deviation of the data points from the fitted curve, eq (1), is also presented.

Table 4 lists, according to the above format, the remaining tables and plots of the conductivity data for each of the specimens tested.

Table 4. Location index for figures and tables of conductivity data for all specimens.

	Tables		Figures		
Specimen Identification	Table of Data	Table of $\lambda(T)$	Linear plot of $\lambda(T)$	Logarithmic plot of $\lambda(T)$	Plot of Deviations
H-003	5				
H-003-R	6	7	5	6	7
HN-003	8	9	8	9	10
MTL-003	10	11	11	12	13
MT-003	12				
MT-003-R	13	14	14	15	16
MT-001	15	16	17	18	19

Dependence of Thermal Conductivity on Temperature

Type H film (unadmixed; neat): The dependence of thermal conductivity on temperature for this unfilled film is plotted in figure 5, with conventional linear axes to clarify the behavior at temperatures above about 100 K; all the data points above this temperature are clearly separated. In figure 6, with logarithmic axes of conductivity and temperature, the data points below 100 K are clearly separated. On both plots, at temperatures below about 30 K the conductivity rises approximately linearly with temperature; the conductivity then levels off to an approximately constant value (190 mW/(m·K)) of conductivity at temperatures above about 300 K. The conductivity at 306 K is about 18 times that at 4.6 K (tables 5 and 6). The maximum positive and negative deviations (fig. 7) of the data from the fitted curve are less than about 4 percent.

Type HN film (unadmixed): At temperatures below about 10 K there is a slight upward concavity in the conductivity function (figs. 8 and 9); otherwise the behavior of the conductivity is qualitatively similar. However, the tendency for the conductivity to become constant at temperatures around 300 K is not as strong; the conductivity at 300 K reaches a value of about 375 mW/(m·K) and is still rising with increasing temperature. The conductivity at 297 K is more than 28 times that at 4.6 K (table 8). The maximum deviations (fig. 10) of the data from the fitted correlation are less than 4.5 percent.

Type MTL film (low alumina content): The behavior (figs. 11 and 12) of this film, with the lower quantity of admixed alumina filler, is similar to that of the type HN film. The conductivity is about 420 mW/(m·K) at 300 K.

The conductivity at 300 K rises to a value about 32 times that at 4.6 K (table 10). The maximum deviations (fig. 13) of the data from the fitted correlation are less than 3 percent.

Type MT film (high alumina content, 76 μm thick): The conductivity of this film, with the higher quantity of admixed alumina filler, behaves similarly (figs. 14 and 15) to that of the types HN and MTL film. The conductivity is about 510 mW/(m·K) at 300 K. The conductivity at 306 K is about 51 times that at 4.6 K (tables 12 and 13). The maximum positive deviation (fig. 16) of the data from the fitted correlation is about 7.5 percent, and the maximum negative deviation is about 5.5 percent.

Type MT film (high alumina content, 25 μm thick): The behavior (figs. 17 and 18) of the conductivity of this film, a thinner version of the preceding specimen, is also similar to that of the types HN and MTL film. The conductivity at about 306 K is about 37 times that at 5.1 K (table 15). The maximum deviations (fig. 19) of the data from the fitted correlation are less than about 3 percent.

The conductivity correlations for the first four specimens of PPMI film, all 76 μm thick, are compared with each other in figures 20 and 21. On the scale used in figure 20, the conductivity of type H (neat; unadmixed) film is nearly constant for temperatures above 200 K, while the conductivities of all the other types (HN, MT and MTL) are still rising with increasing temperature. As we might expect, the introduction of alumina filler into the PPMI film increased the thermal conductivity. The type MT film (high alumina content) has the greatest conductivity of the four types of film. Surprisingly, the conductivity of the type HN (neat) film is more similar to those of the alumina-filled films than to that of the type H (neat) film.

The large difference observed between the H and HN specimens was not expected. However, these two specimen types are made by different processes. The details of their manufacture are proprietary and are not available to NIST. The measurements on PPMI film H-003 were reproducible within the experimental imprecision of the apparatus.

Reproducibility of Tests

The reproducibility of thermal conductivity measurements on PPMI film was tested by constructing two separate specimen stacks of type H film (H-003 and H-003-R, both 76 μm thick). Identical procedures were followed (cutting, greasing, compressing and mounting into the apparatus) in constructing the two specimens. A similar test of repeatability was carried out on two specimen stacks of type MT film (MT-003 and MT-003-R, both 76 μm). For each of these two types of film the conductivity-temperature function of one was not appreciably different from that of the other. Therefore, as indicated in table 4, for each of these two types of film (type H, tables 5 and 6; type MT, tables 12 and 13) both tests were analyzed together on the same graphs (type H: figs. 5 through 7; type MT: figs. 14 to 16).

Dependence of Thermal Conductivity on Film Thickness

The thermal conductivities of the PPMI specimens MT-001 and MT-003 show no observable dependence on the film thickness. Figure 22 shows the thermal conductivity as a function of temperature for both MT-001 and MT-003. The deviation plot in figure 23 compares the experimental data for both MT-001 and MT-003 to the polynomial obtained by a least-squares fit of the MT-003 data alone. Differences in the observed thermal conductivities for the two different film types at temperatures above 20 K are within experimental imprecision. The reason for the large deviation in the data for the MT-001 specimen at temperatures below 20 K (fig. 23) is not known.

Effect of Thermal Contact Resistance

By analogy with electrical resistance, we define the total thermal resistance $\Delta T/Q$ of a stacked-film specimen as the total difference in temperature $\Delta T = T_{hot} - T_{cold}$ between the outer specimen surfaces divided by the total heat Q passing through the specimen. The nominal "thermal resistance per film layer" is the total resistance divided by the number of layers of film in the specimen stack. It includes the intrinsic thermal resistance of the film layer alone plus the thermal resistances of the two adjoining half-layers of grease.

A series of measurements was performed to determine the difference between the thermal resistance per film layer as defined above for specimens made with ungreased (dry) contacts and the resistance per layer for those made with all contacts greased. This difference in thermal resistance was examined for dependence on the number of interfacial contacts. Thermal resistance was measured at a mean specimen temperature of 277.5 K. The specimens were constructed from 60, 84, 85 and 100 layers of 76-μm MT film (MT-003: 76 μm, 0.003 in), and from 252 layers of 25-μm (MT-001: 25 μm, 0.001 in) film. The number 252 was chosen because the thickness of 252 layers of 25-μm film equals that of 84 layers of 76-μm film. The results, expressed as thermal contact resistance per layer as a function of number of contacts (interfaces) are shown in figure 24. (Measurement of one partially greased specimen was also attempted but the results strongly suggested that gross contamination of the dry interfaces occurred during the process of constructing the specimen within the retaining tube.)

An attempt was made to measure the thickness of the grease introduced between each of the film layers in the MT-001 specimen. This was done by measuring the total thickness of a compressed specimen stack and dividing by the total number of film layers in the specimen, both for a greased stack and for a dry (ungreased) stack. The resulting thickness for a greased specimen stack is that of one layer of film plus the thickness of the associated two (half) grease films. The uncertainty of measurements of thickness was less than 12 μm (0.0005 in). There was no measurable difference in total thickness (within ≈12 μm) between a specimen stack composed of 252 layers of 25 μm (dry) film and the same specimen after it was reformed with (251 internal plus 2 external) fully greased interfaces. The 253 greased interfaces added negligible thickness to the that of the whole specimen stack, so the thickness of a single film of grease is also negligible in comparison to the

thickness of the associated PPMI film. The surface roughness of this film was comparable to that of the other filled films and was much rougher than the unfilled films.

The specimen with 252 layers of 25-μm (MT-001: 0.001 in) film was constructed so as to have the same total thickness as those with 84 (252/3) layers of 76-μm (MT-003: 0.003 in) film. However, the number of greased interfaces for the 252-layer specimen was about three times the number of interfaces for 84-layer specimens, with comparable surface roughnesses. As figure 24 shows, the scaled thermal resistance per layer for the 252-layer specimen of MT-001 agrees with the values of thermal resistance per layer for the 84-layer specimens of MT-003 film, within experimental uncertainty. This result demonstrates that the resistance, conductance, and conductivity are independent of thickness, and that the contact resistance, for greased interfaces, is negligible.

For the range of number of layers shown in figure 24, the mean value of thermal resistance per layer for the greased 76-μm specimens is 0.52 K/W. This is the probable value of the resistance per greased layer. The straight line is a least-squares fit to the points for greased interfaces. The open circle shown in figure 24 at 84 layers, 0.66 K/W, lies 0.14 K/W (27 percent) higher than the line; because the contact resistance of a greased interface is negligible, this difference represents the contact resistance of a dry interface.

Dependence of Conductivity on Applied Pressure

Thermal contact resistance is reasonably expected to depend on applied pressure; the intrinsic thermal resistance of a PPMI layer should be only a weak function of applied pressure over the range of pressure used. An important question is whether the maximum clamping pressure, 17 MPa, applied to each specimen during the investigation described above was sufficient to remove the effect of thermal contact resistance. To determine the effect of pressure on total thermal resistance of a specimen stack, a third specimen of film type MT-003 was constructed, and the total resistance measured, for five different values of clamping pressure ranging from 5 to 17 MPa. The dependence of resistance on pressure, listed in table 17, was measured for three different mean specimen temperatures: 277.8 K (ice), 80.3 K (LN), and 8.3 K (LHe). Figure 25 illustrates that for all three mean temperatures the total thermal resistance $\Delta T/Q$ per layer of film appears to become independent of applied pressure above about 12 MPa (1.7 kpsi); therefore the computed thermal conductivity is also independent of pressure (fig. 26). Above this threshold pressure (12 MPa), the contact resistance at ice and liquid nitrogen was less than 1 percent, and at liquid helium, 3 percent. Within the "saturation" region of thermal resistance, at pressures above 12 MPa, the standard deviations of the residuals of the points about the "level" portion of the curve are, for 277.8 K (ice bath), 0.6 percent; for 80.3 K (LN bath), 0.5 percent; and for 8.3 K (LHe), 3 percent.

Effect of Heat Treatment on Conductivity

An important application of this PPMI film is to provide electrical insulation between layers of copper wire in a superconducting magnet. In such use the PPMI film may be installed between the layers of magnet wire. At the completion of the assembly the magnet is thermally cured for 90 minutes at about 425 K (150°C). An important question was whether the thermal conductivity of this PPMI film would be changed by undergoing a heat treatment similar to that typically used in the application just described. The film could also be subjected to a mechanical pressure of about 69 MPa (10 kpsi) during this heat treatment.

A PPMI film specimen was heat-treated to simulate these conditions. An ungreased stack of 33 layers of HN-003 film was mounted and compressed between two copper plates similar to those between which the specimen is mounted in the conductivity apparatus. Compression bolts produced a mechanical pressure of 69 MPa (10 kpsi) on the specimen. The assembly was then placed in an oven at constant temperature and heated to a temperature of 150°C. This temperature was maintained within ±1°C for 90 minutes, after which the oven and stack were then allowed to cool slowly. The layers of film were separated, greased, and restacked. This specimen was then retested to determine whether there was any noticeable change in its thermal resistance due to the heat treatment. The resulting data are identified as "HN-Heat" in table 18.

Values of thermal resistance of the HN film before and after heat treatment were in agreement within the experimental reproducibility of the apparatus. Figure 27 shows the thermal conductivity as a function of temperature for specimens HN-003 and HN-Heat. The deviation plot in figure 28 compares experimental data for HN-003 and HN-Heat to the polynomial obtained from a least-squares fit for the data for HN-003 alone.

COMPARISON WITH RESULTS FROM OTHER STUDIES

In figure 29 we compare results from the literature of measurements of thermal conductivity of similar insulating films from other studies. Measurements of Kapton PPMI (Refs. 6, 12-15) and of polyester-amide-imide (PEAI; Ref. 17) films are shown as crosses. Results for Vespel (Refs. 7, 10) and Kerimid (Ref. 8), castable forms of PPMI, are plotted as filled circles and a filled square. It is of possible interest to compare measurements under similar conditions for polyethylene (PE) tapes and for Mylar (PET) films, even though these materials are not PPMI. The results for PE tapes (Ref. 11) are plotted as a long rectangle, and those for PET films (Refs. 16, 18) are given as filled triangles.

Measurements from Refs. 6 and 14 on neat Kapton, from Ref. 8 on neat Kerimid, and from Ref. 11 on PE, and one of the results from Ref. 17 on PEAI, diverge by a factor of two or more from the results of this study. The remaining measurements (Refs. 7 and 10 on neat Vespel; Refs. 12, 13 and 15 on PPMI; Refs. 16 and 18 on PET; and Ref. 17 on PEAI) agree well, collectively, with the results represented by the lowest curve (specimen H-003) of figure 29, considering the experimental imprecision of the apparatus used in this work and the spread in the results from the other studies.

SUMMARY

Specimens of PPMI film were made by stacking multiple layers of film together. Conductive grease was used to reduce thermal contact resistance between the layers of film. We found evidence which showed that the total thermal resistance of the interstitial grease films was negligible. A sufficient amount of pressure was applied to the specimen stack to minimize contact resistance.

Thermal conductivity of the PPMI film was measured for mean specimen temperatures ranging from 4 to 308 K. The inaccuracy of data obtained with the fixed-point apparatus used to measure conductivity is estimated to be about ±5 percent. Correlations were obtained by use of a least-squares fit to the integral of a fourth-order polynomial in $\ell n(T+1)$ used to represent the conductivity function. The standard deviations of the residual between the data and the fitted functions are typically about ±3 percent.

The thermal conductivities of the PPMI film specimens MT-001 and MT-003 (high alumina content; thicknesses of 25 μm and 76 μm) show no observable dependence on the film thickness. The presence of alumina particles had a large effect on the thermal conductivity, which increased directly with the content of alumina. The size and number density of the alumina particle filler is unavailable from the manufacturer.

Heat treatment at 150°C for a period of 90 minutes had no noticeable effect on the observed thermal conductivity of a specimen of PPMI film HN-003.

ACKNOWLEDGMENTS

This work was supported in part under contract 4555510 through P. Limon of the Superconducting Supercollider (SSC) Central Design Group, Lawrence Berkeley Laboratories, Berkeley, California; and through R. Carcagno of the SSC Accelerator Systems Division, Universities Research Association, Inc., Dallas, Texas. The specimens were donated through D. J. Parish, and technical information on polyimide film processing was given by J. Ochsner, both of the DuPont Company. M.B. Rhodes of the Optical Microscopy Laboratory, University of Massachusetts at Amherst, advised us on microscopic study of the differences between PPMI films. Measurements of surface roughness were made by P. Rice of the Electromagnetic Technology Division of NIST-Boulder.

Table 5. Experimental conductivity as a function of temperature for PPMI film H-003.

ΔT Setting	Average Temperature Kelvin	Thermal Conductivity W/(m·K)	Cold Bath
1	4.638	0.011	LHe
2	5.159	0.011	
4	6.224	0.014	
8	8.375	0.019	
16	12.902	0.031	
32	22.493	0.053	
64	41.924	0.086	
2	77.091	0.126	LN_2
2	77.093	0.127	
4	78.184	0.126	
8	80.373	0.129	
16	84.769	0.132	
32	93.618	0.138	
64	111.507	0.147	
75	117.724	0.151	
1	192.585	0.173	CO_2-alcohol
2	193.168	0.171	
4	194.335	0.170	
8	196.684	0.174	
16	201.395	0.175	
32	210.876	0.176	
64	230.124	0.178	
1	273.734	0.183	Ice-water
2	274.319	0.184	
2	274.319	0.184	
4	275.490	0.185	
8	277.836	0.186	
16	282.553	0.188	
32	292.061	0.190	
32	292.066	0.190	
55.8	306.424	0.192	
56.1	306.611	0.192	

Table 6. Experimental conductivity as a function of temperature for PPMI film H-003-R (retest).

ΔT Setting	Average Temperature Kelvin	Thermal Conductivity W/(m·K)	Cold Bath
1	4.637	0.011	LHe
8	8.373	0.019	
32	22.465	0.053	
8	80.367	0.128	LN_2
16	84.754	0.132	
32	93.580	0.137	
64	111.433	0.147	
8	196.691	0.180	CO_2-alcohol
32	210.969	0.188	
2	274.320	0.191	Ice-water
8	277.841	0.192	
32	292.073	0.195	
56	306.526	0.198	

Table 7. Thermal conductivity values as a function of temperature for specimen PPMI film H-003.

T, K	λ(T), W/(m·K)	T, K	λ(T), W/(m·K)	T, K	λ(T), W/(m·K)	T, K	λ(T), W/(m·K)
4.10	0.009	9.10	0.022	51.00	0.100	110.00	0.148
4.20	0.009	9.20	0.022	52.00	0.101	120.00	0.153
4.30	0.010	9.30	0.022	53.00	0.102	130.00	0.157
4.40	0.010	9.40	0.022	54.00	0.103	140.00	0.161
4.50	0.010	9.50	0.023	55.00	0.105	150.00	0.165
4.60	0.010	9.60	0.023	56.00	0.106	160.00	0.168
4.70	0.010	9.70	0.023	57.00	0.107	170.00	0.171
4.80	0.011	9.80	0.024	58.00	0.108	180.00	0.173
4.90	0.011	9.90	0.024	59.00	0.109	190.00	0.176
5.00	0.011	10.00	0.024	60.00	0.110	200.00	0.178
5.10	0.011	11.00	0.027	61.00	0.111	210.00	0.180
5.20	0.012	12.00	0.029	62.00	0.112	220.00	0.181
5.30	0.012	13.00	0.032	63.00	0.113	230.00	0.183
5.40	0.012	14.00	0.035	64.00	0.114	240.00	0.184
5.50	0.012	15.00	0.037	65.00	0.115	250.00	0.185
5.60	0.012	16.00	0.039	66.00	0.116	260.00	0.186
5.70	0.013	17.00	0.042	67.00	0.117	270.00	0.187
5.80	0.013	18.00	0.044	68.00	0.118	280.00	0.188
5.90	0.013	19.00	0.047	69.00	0.119	290.00	0.189
6.00	0.013	20.00	0.049	70.00	0.120	300.00	0.189
6.10	0.014	21.00	0.051	71.00	0.121	310.00	0.190
6.20	0.014	22.00	0.053	72.00	0.121	320.00	0.190
6.30	0.014	23.00	0.055	73.00	0.122	330.00	0.190
6.40	0.014	24.00	0.057	74.00	0.123		
6.50	0.015	25.00	0.059	75.00	0.124		
6.60	0.015	26.00	0.061	76.00	0.125		
6.70	0.015	27.00	0.063	77.00	0.126		
6.80	0.016	28.00	0.065	78.00	0.126		
6.90	0.016	29.00	0.067	79.00	0.127		
7.00	0.016	30.00	0.069	80.00	0.128		
7.10	0.016	31.00	0.071	81.00	0.129		
7.20	0.017	32.00	0.072	82.00	0.130		
7.30	0.017	33.00	0.074	83.00	0.130		
7.40	0.017	34.00	0.076	84.00	0.131		
7.50	0.017	35.00	0.077	85.00	0.132		
7.60	0.018	36.00	0.079	86.00	0.133		
7.70	0.018	37.00	0.081	87.00	0.133		
7.80	0.018	38.00	0.082	88.00	0.134		
7.90	0.018	39.00	0.084	89.00	0.135		
8.00	0.019	40.00	0.085	90.00	0.135		
8.10	0.019	41.00	0.087	91.00	0.136		
8.20	0.019	42.00	0.088	92.00	0.137		
8.30	0.019	43.00	0.089	93.00	0.137		
8.40	0.020	44.00	0.091	94.00	0.138		
8.50	0.020	45.00	0.092	95.00	0.139		
8.60	0.020	46.00	0.094	96.00	0.139		
8.70	0.021	47.00	0.095	97.00	0.140		
8.80	0.021	48.00	0.096	98.00	0.141		
8.90	0.021	49.00	0.097	99.00	0.141		
9.00	0.021	50.00	0.099	100.00	0.142		

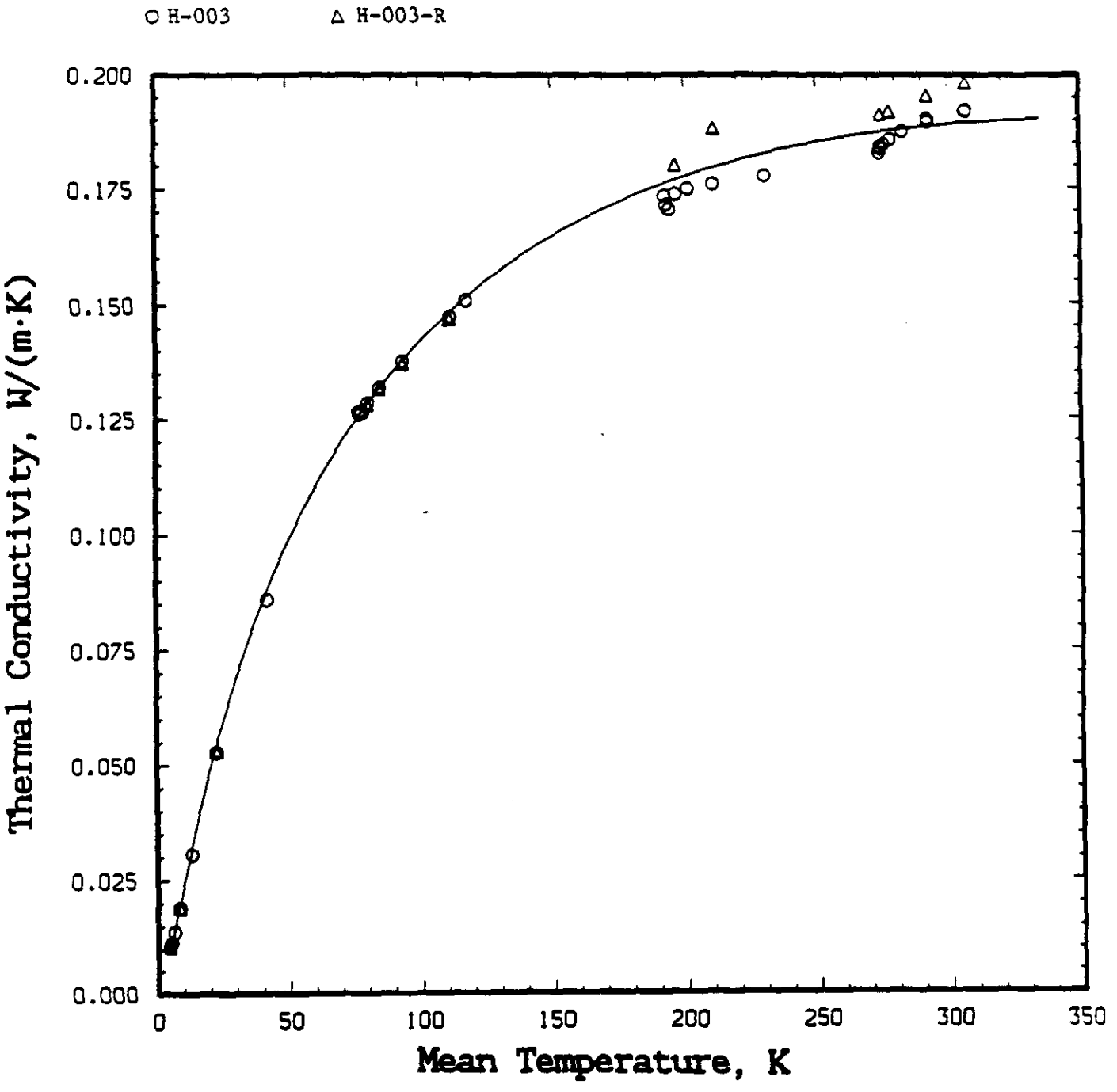

Figure 5. Thermal conductivity of PPMI film specimen H-003 and H-003-R (repeated measurements on same specimen). Experimental data are presented as discrete points. Two specimens were tested to determine reproducibility. Both scales are linear, which clarifies the behavior at high temperatures.

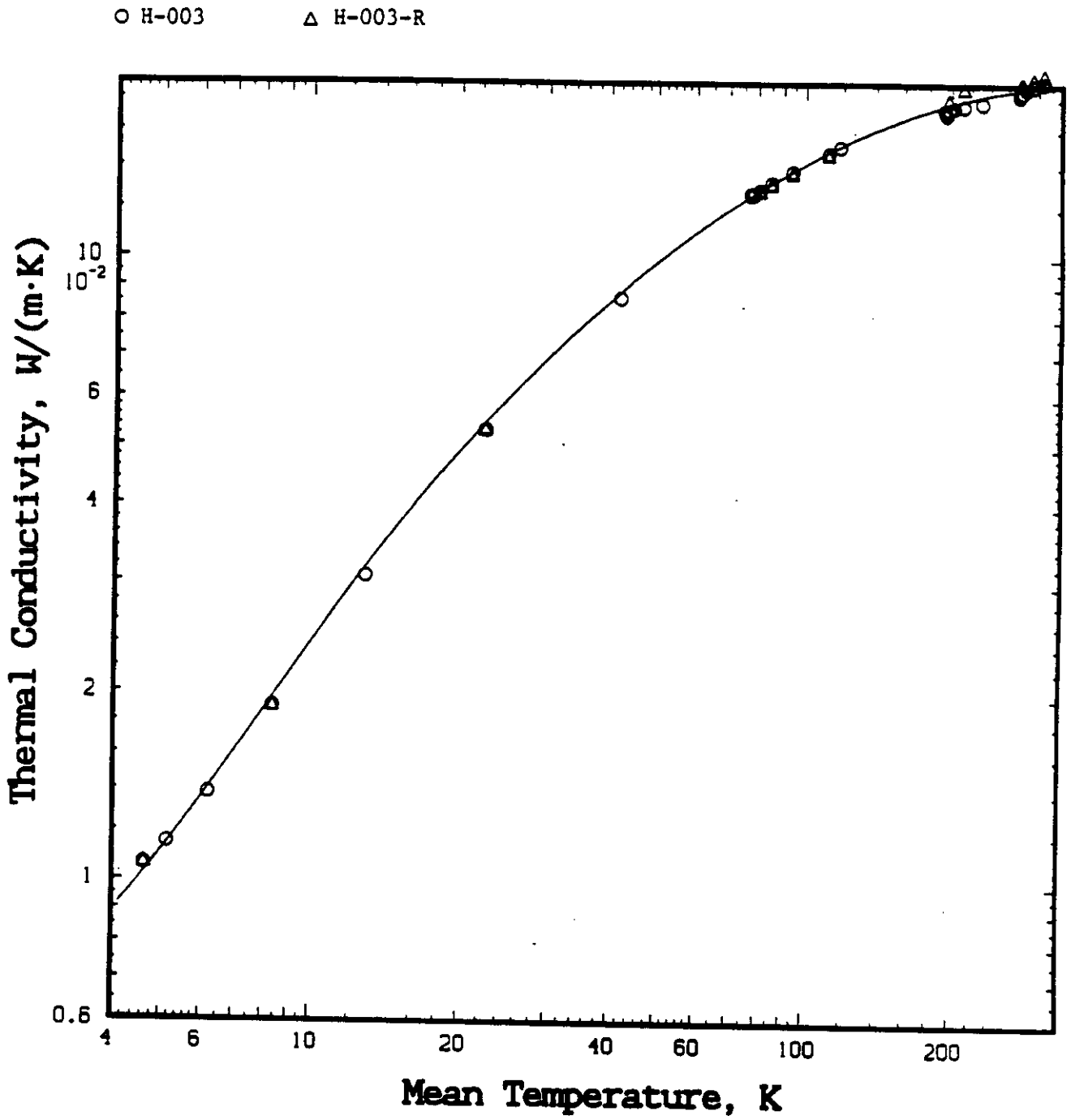

Figure 6. Thermal conductivity of PPMI film specimen H-003 and H-003-R (repeated measurements on same specimen). Experimental data are presented as discrete points. Two specimens were tested to determine reproducibility. Both scales are logarithmic, which clarifies the behavior at low temperatures.

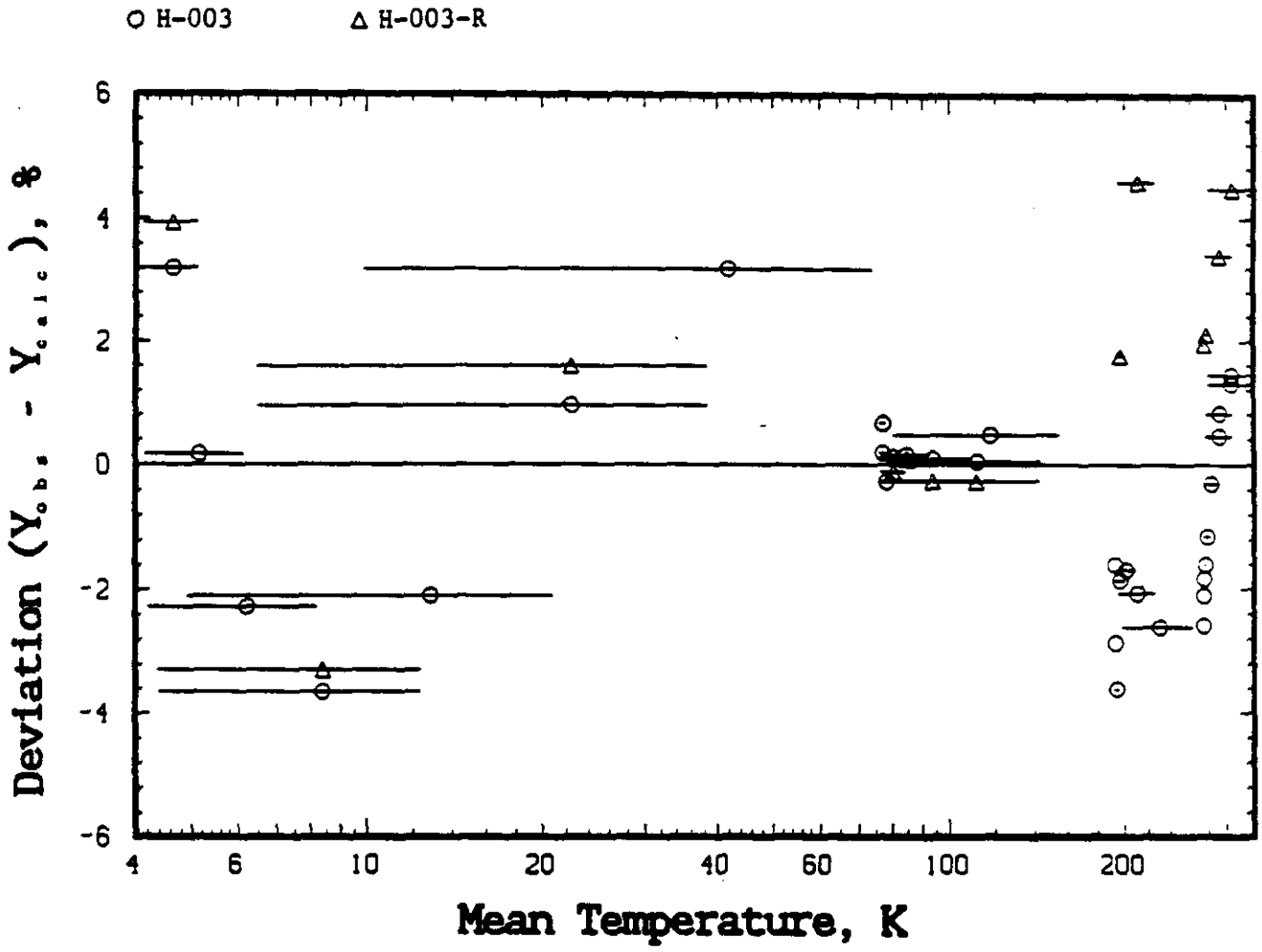

Figure 7. Relative deviations of experimental and calculated thermal conductivity integrals for PPMI film specimen H-003 and H-003-R (repeated measurements on same specimen). The horizontal bar indicates the span of temperature used for each run.

Table 8. Experimental conductivity as a function of temperature for PPMI film HN-003.

ΔT Setting	Average Temperature Kelvin	Thermal Conductivity W/(m·K)	Cold Bath
1	4.641	0.013	LHe
2	5.166	0.014	
4	6.236	0.017	
8	8.437	0.024	
16	13.125	0.039	
32	23.027	0.069	
1	76.566	0.188	LN_2
4	78.271	0.194	
8	80.551	0.197	
16	85.143	0.204	
32	94.434	0.217	
64	113.410	0.240	
1	192.638	0.314	CO_2-alcohol
2	193.275	0.312	
4	194.558	0.317	
8	197.143	0.325	
16	202.287	0.321	
32	212.921	0.344	
44.5	221.262	0.350	
1	273.784	0.358	Ice-water
2	274.419	0.359	
4	275.692	0.361	
8	278.246	0.364	
16	283.384	0.368	
32	293.783	0.376	
37.6	297.360	0.369	

Table 9. Thermal conductivity values as a function of temperature for specimen PPMI film HN-003.

T, K	λ(T) W/(m·K)	T K	λ(T) W/(m·K)	T K	λ(T) W/(m·K)	T K	λ(T) W/(m·K)
4.10	0.012	9.10	0.025	51.00	0.143	110.00	0.238
4.20	0.012	9.20	0.025	52.00	0.145	120.00	0.250
4.30	0.012	9.30	0.025	53.00	0.148	130.00	0.261
4.40	0.012	9.40	0.026	54.00	0.150	140.00	0.271
4.50	0.012	9.50	0.026	55.00	0.152	150.00	0.281
4.60	0.013	9.60	0.026	56.00	0.154	160.00	0.290
4.70	0.013	9.70	0.027	57.00	0.156	170.00	0.298
4.80	0.013	9.80	0.027	58.00	0.158	180.00	0.306
4.90	0.013	9.90	0.027	59.00	0.160	190.00	0.314
5.00	0.013	10.00	0.028	60.00	0.162	200.00	0.321
5.10	0.014	11.00	0.031	61.00	0.164	210.00	0.328
5.20	0.014	12.00	0.034	62.00	0.166	220.00	0.334
5.30	0.014	13.00	0.038	63.00	0.167	230.00	0.340
5.40	0.014	14.00	0.041	64.00	0.169	240.00	0.346
5.50	0.015	15.00	0.045	65.00	0.171	250.00	0.352
5.60	0.015	16.00	0.048	66.00	0.173	260.00	0.357
5.70	0.015	17.00	0.051	67.00	0.175	270.00	0.362
5.80	0.015	18.00	0.055	68.00	0.177	280.00	0.367
5.90	0.016	19.00	0.058	69.00	0.178	290.00	0.372
6.00	0.016	20.00	0.061	70.00	0.180	300.00	0.376
6.10	0.016	21.00	0.064	71.00	0.182	310.00	0.381
6.20	0.016	22.00	0.068	72.00	0.183		
6.30	0.017	23.00	0.071	73.00	0.185		
6.40	0.017	24.00	0.074	74.00	0.187		
6.50	0.017	25.00	0.077	75.00	0.189		
6.60	0.017	26.00	0.080	76.00	0.190		
6.70	0.018	27.00	0.083	77.00	0.192		
6.80	0.018	28.00	0.086	78.00	0.193		
6.90	0.018	29.00	0.089	79.00	0.195		
7.00	0.018	30.00	0.092	80.00	0.197		
7.10	0.019	31.00	0.094	81.00	0.198		
7.20	0.019	32.00	0.097	82.00	0.200		
7.30	0.019	33.00	0.100	83.00	0.201		
7.40	0.020	34.00	0.103	84.00	0.203		
7.50	0.020	35.00	0.105	85.00	0.204		
7.60	0.020	36.00	0.108	86.00	0.206		
7.70	0.020	37.00	0.110	87.00	0.207		
7.80	0.021	38.00	0.113	88.00	0.209		
7.90	0.021	39.00	0.115	89.00	0.210		
8.00	0.021	40.00	0.118	90.00	0.212		
8.10	0.022	41.00	0.120	91.00	0.213		
8.20	0.022	42.00	0.123	92.00	0.215		
8.30	0.022	43.00	0.125	93.00	0.216		
8.40	0.023	44.00	0.128	94.00	0.217		
8.50	0.023	45.00	0.130	95.00	0.219		
8.60	0.023	46.00	0.132	96.00	0.220		
8.70	0.024	47.00	0.134	97.00	0.222		
8.80	0.024	48.00	0.137	98.00	0.223		
8.90	0.024	49.00	0.139	99.00	0.224		
9.00	0.025	50.00	0.141	100.00	0.226		

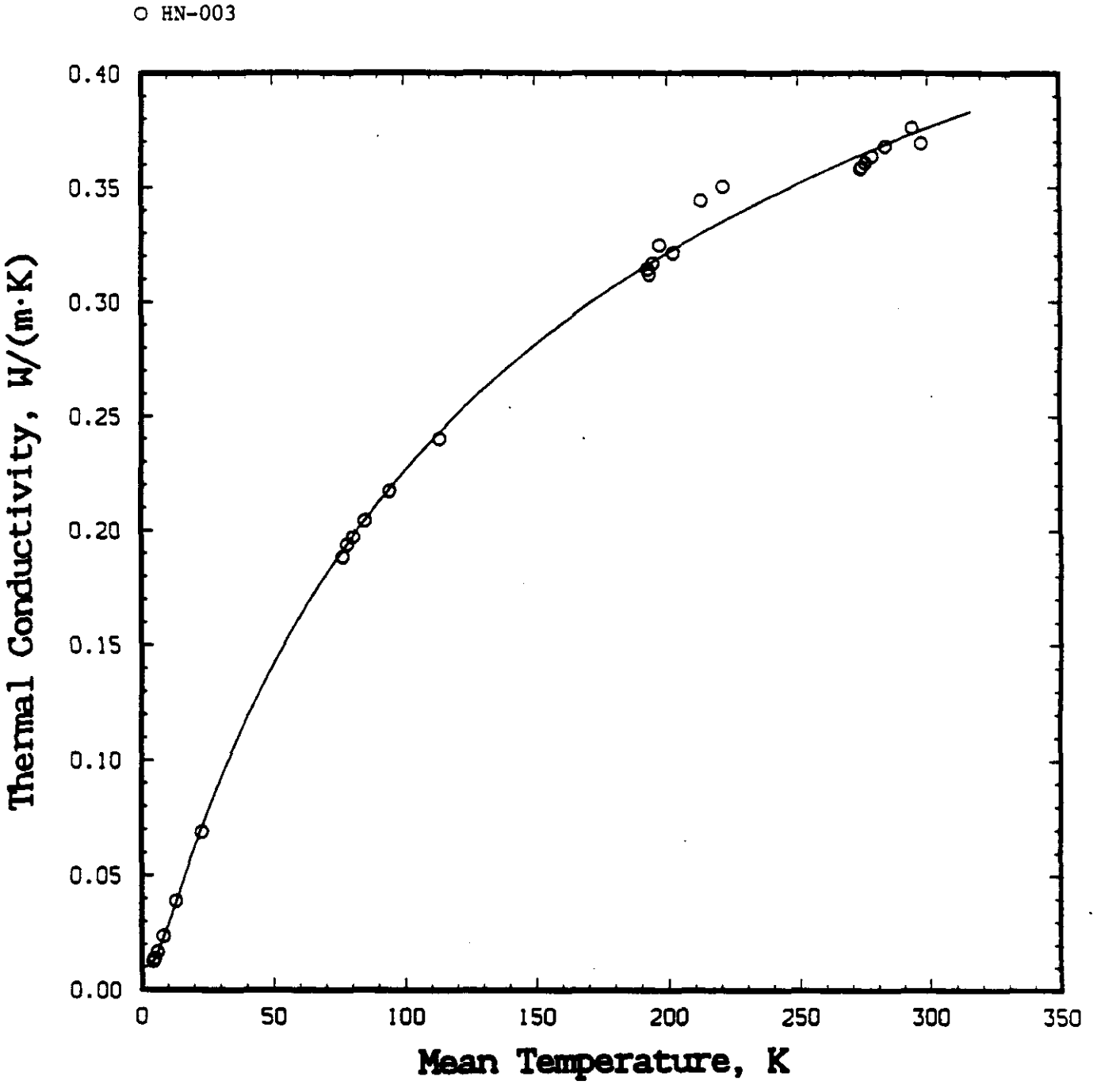

Figure 8. Thermal conductivity of PPMI film specimen HN-003. Experimental data are presented as discrete points. Both scales are linear, which clarifies the behavior at high temperatures.

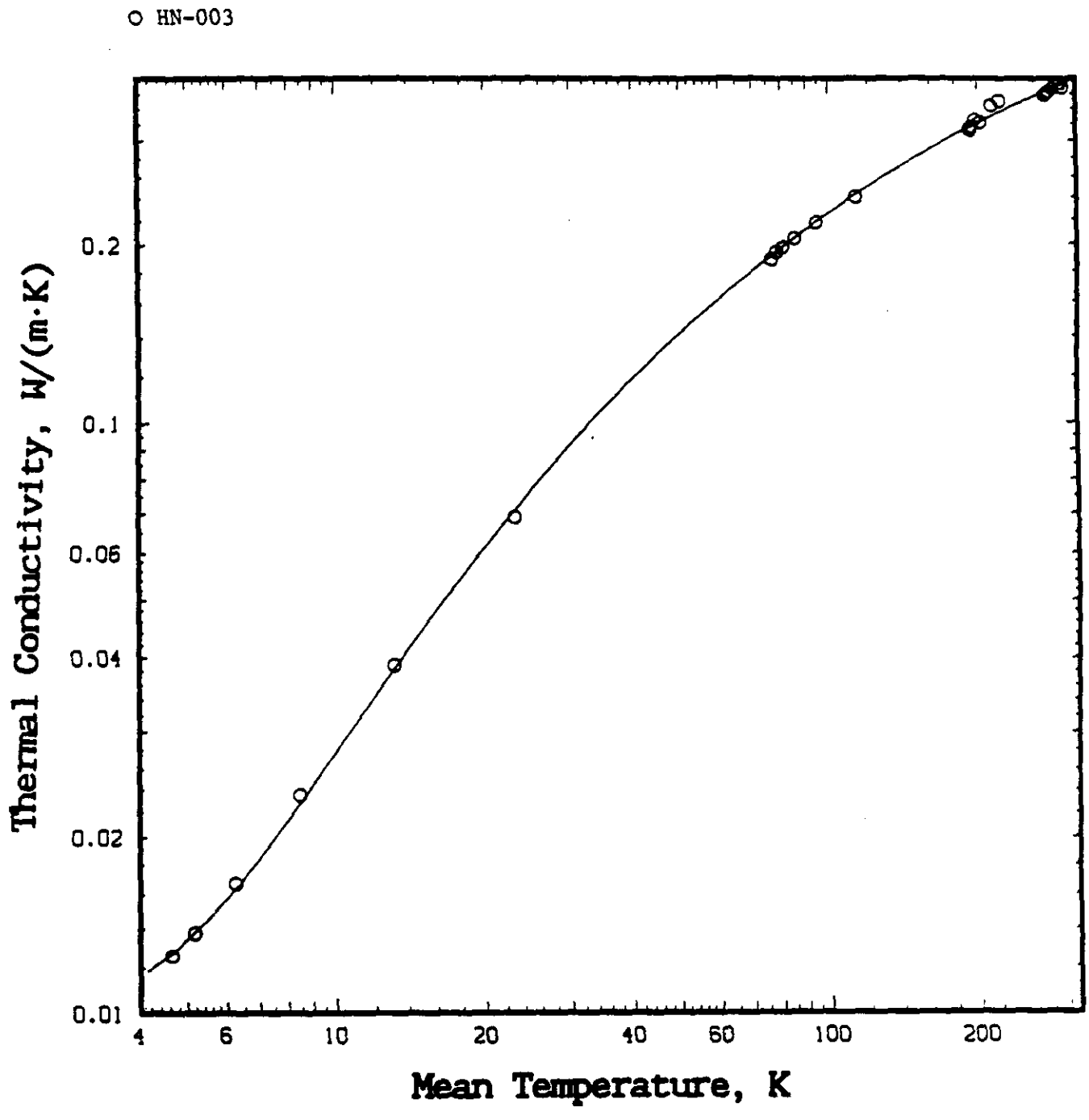

Figure 9. Thermal conductivity of PPMI film specimen HN-003. Experimental data are presented as discrete points. Both scales are logarithmic, which clarifies the behavior at low temperatures.

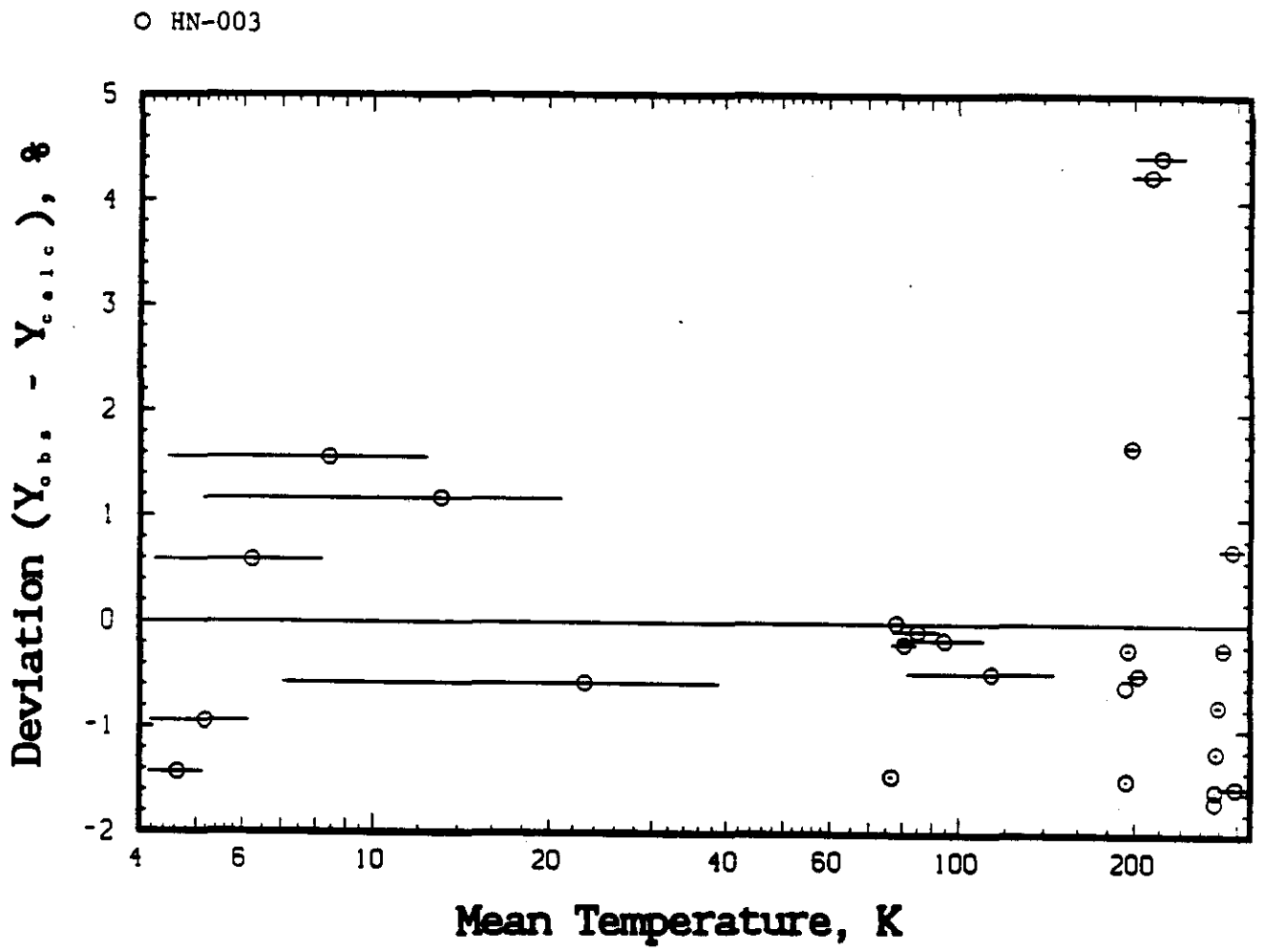

Figure 10. Relative deviations of experimental and calculated thermal conductivity integrals for PPMI film specimen HN-003. The horizontal bar indicates the span of temperature for each run.

Table 10. Experimental conductivity as a function of temperature for PPMI film MTL-003.

ΔT Setting	Average Temperature Kelvin	Thermal Conductivity W/(m·K)	Cold Bath
1	4.636	0.013	LHe
2	5.154	0.014	
4	6.214	0.018	
8	8.359	0.026	
16	12.908	0.043	
32	22.519	0.079	
63.6	42.026	0.138	
8	80.438	0.227	LN_2
16	84.906	0.235	
32	93.924	0.248	
64	112.250	0.272	
4	194.455	0.371	CO_2-alcohol
8	196.911	0.369	
16	201.834	0.367	
32	211.848	0.381	
55.7	226.853	0.388	
1	273.759	0.401	Ice-water
2	274.368	0.401	
4	275.589	0.403	
8	278.038	0.406	
16	282.957	0.410	
32	292.892	0.416	
44	300.369	0.420	

Table 11. Thermal conductivity values as a function of temperature for specimen PPMI film MTL-003.

T K	λ(T) W/(m·K)	T K	λ(T) W/(m·K)	T K	λ(T) W/(m·K)	T K	λ(T) W/(m·K)
4.10	0.012	9.10	0.028	51.00	0.167	110.00	0.275
4.20	0.012	9.20	0.028	52.00	0.170	120.00	0.288
4.30	0.012	9.30	0.028	53.00	0.172	130.00	0.300
4.40	0.013	9.40	0.029	54.00	0.175	140.00	0.311
4.50	0.013	9.50	0.029	55.00	0.177	150.00	0.321
4.60	0.013	9.60	0.030	56.00	0.179	160.00	0.331
4.70	0.013	9.70	0.030	57.00	0.182	170.00	0.340
4.80	0.014	9.80	0.030	58.00	0.184	180.00	0.349
4.90	0.014	9.90	0.031	59.00	0.186	190.00	0.357
5.00	0.014	10.00	0.031	60.00	0.188	200.00	0.364
5.10	0.014	11.00	0.035	61.00	0.191	210.00	0.371
5.20	0.014	12.00	0.039	62.00	0.193	220.00	0.378
5.30	0.015	13.00	0.043	63.00	0.195	230.00	0.384
5.40	0.015	14.00	0.047	64.00	0.197	240.00	0.390
5.50	0.015	15.00	0.051	65.00	0.199	250.00	0.396
5.60	0.016	16.00	0.055	66.00	0.201	260.00	0.401
5.70	0.016	17.00	0.059	67.00	0.203	270.00	0.406
5.80	0.016	18.00	0.063	68.00	0.205	280.00	0.411
5.90	0.016	19.00	0.067	69.00	0.207	290.00	0.415
6.00	0.017	20.00	0.071	70.00	0.209	300.00	0.420
6.10	0.017	21.00	0.075	71.00	0.211	310.00	0.424
6.20	0.017	22.00	0.079	72.00	0.213	320.00	0.428
6.30	0.018	23.00	0.082	73.00	0.215		
6.40	0.018	24.00	0.086	74.00	0.217		
6.50	0.018	25.00	0.090	75.00	0.219		
6.60	0.019	26.00	0.093	76.00	0.221		
6.70	0.019	27.00	0.097	77.00	0.223		
6.80	0.019	28.00	0.100	78.00	0.225		
6.90	0.020	29.00	0.104	79.00	0.226		
7.00	0.020	30.00	0.107	80.00	0.228		
7.10	0.020	31.00	0.110	81.00	0.230		
7.20	0.021	32.00	0.113	82.00	0.232		
7.30	0.021	33.00	0.117	83.00	0.233		
7.40	0.021	34.00	0.120	84.00	0.235		
7.50	0.022	35.00	0.123	85.00	0.237		
7.60	0.022	36.00	0.126	86.00	0.239		
7.70	0.022	37.00	0.129	87.00	0.240		
7.80	0.023	38.00	0.132	88.00	0.242		
7.90	0.023	39.00	0.135	89.00	0.244		
8.00	0.023	40.00	0.138	90.00	0.245		
8.10	0.024	41.00	0.141	91.00	0.247		
8.20	0.024	42.00	0.143	92.00	0.248		
8.30	0.025	43.00	0.146	93.00	0.250		
8.40	0.025	44.00	0.149	94.00	0.252		
8.50	0.025	45.00	0.152	95.00	0.253		
8.60	0.026	46.00	0.154	96.00	0.255		
8.70	0.026	47.00	0.157	97.00	0.256		
8.80	0.026	48.00	0.160	98.00	0.258		
8.90	0.027	49.00	0.162	99.00	0.259		
9.00	0.027	50.00	0.165	100.00	0.261		

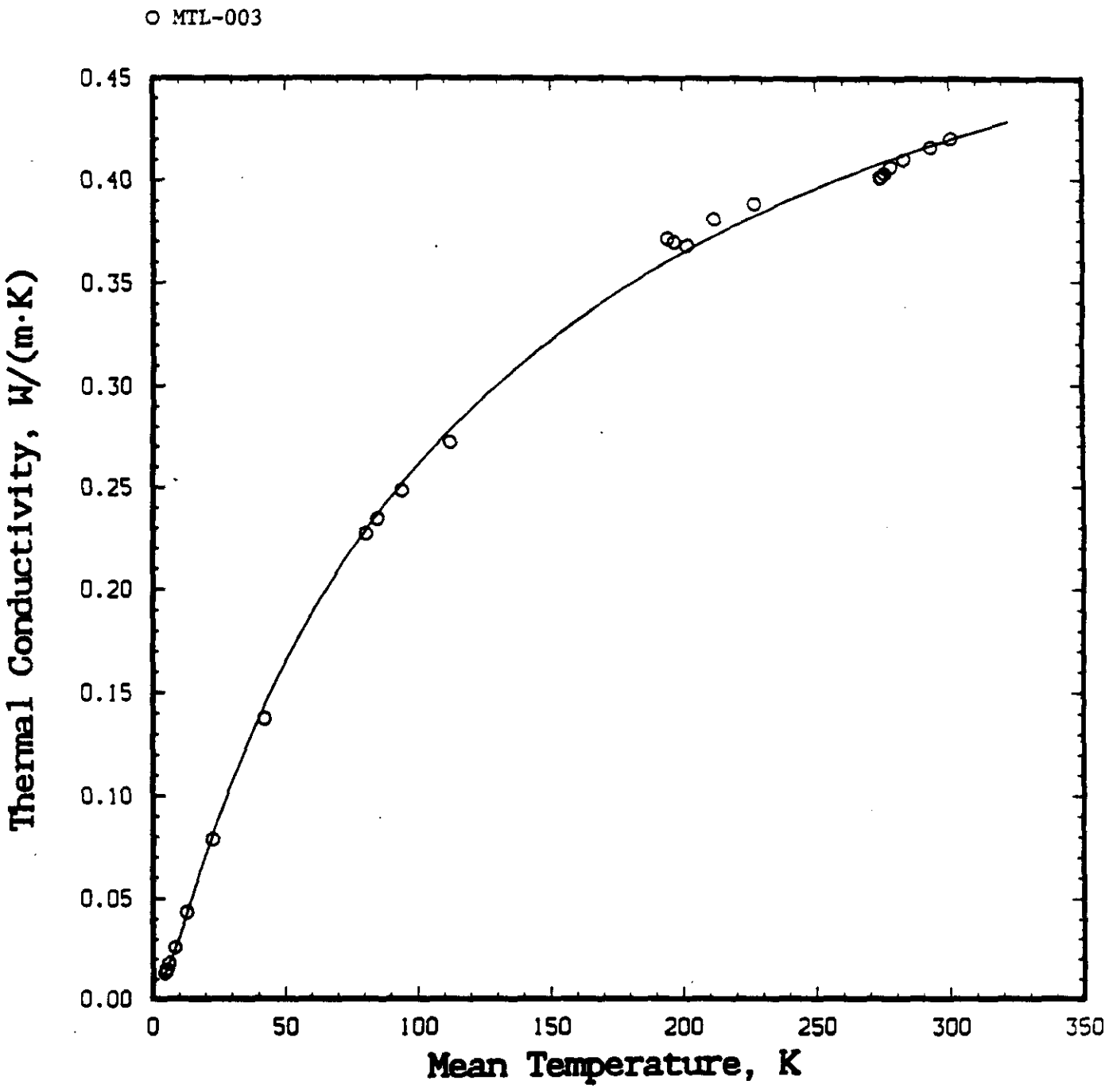

Figure 11. Thermal conductivity of PPMI film specimen MTL-003. Experimental data are presented as discrete points. Both scales are linear, which clarifies the behavior at high temperatures.

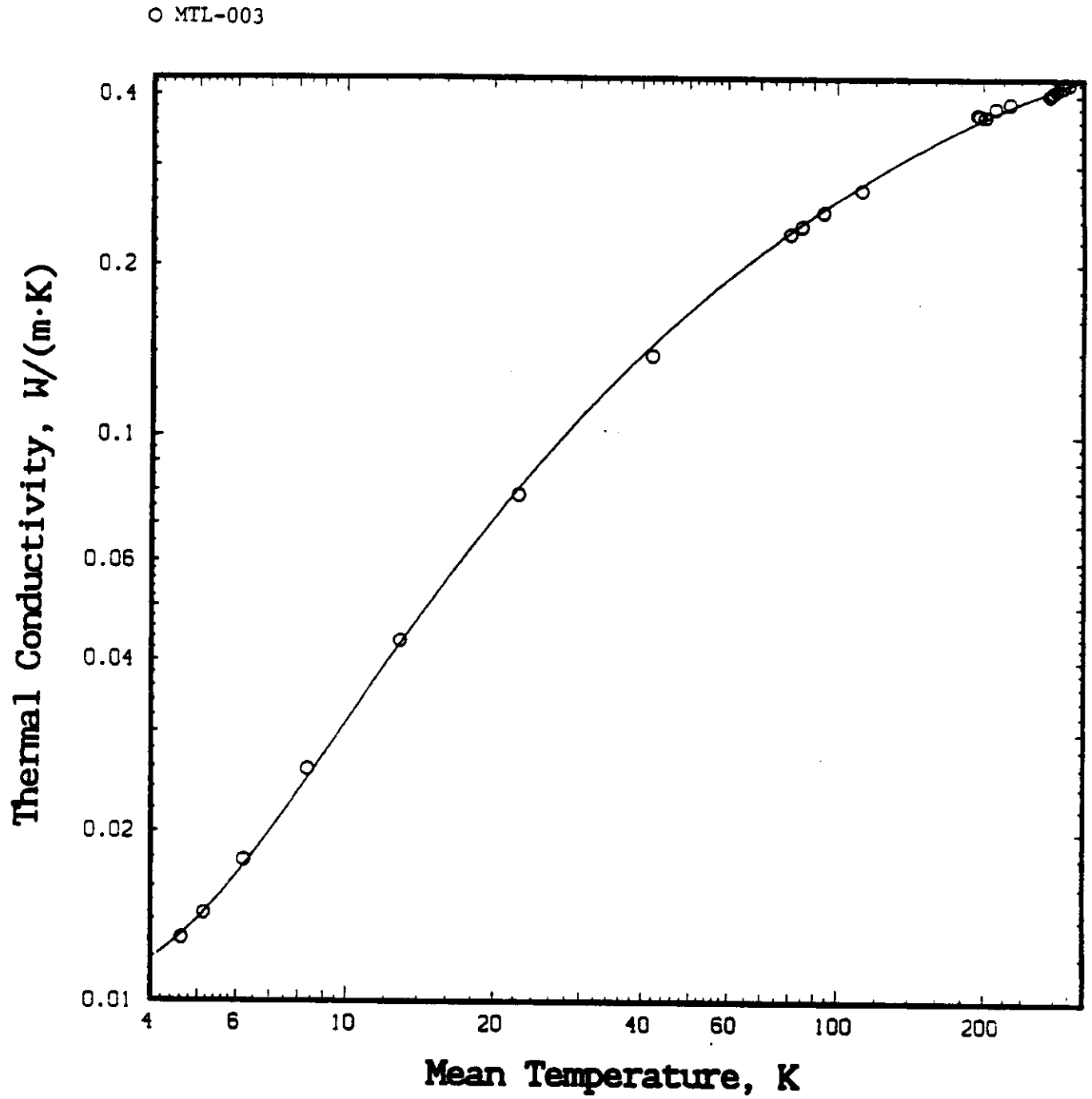

Figure 12. Thermal conductivity of PPMI film specimen MTL-003. Experimental data are presented as discrete points. Both scales are logarithmic, which clarifies the behavior at low temperatures.

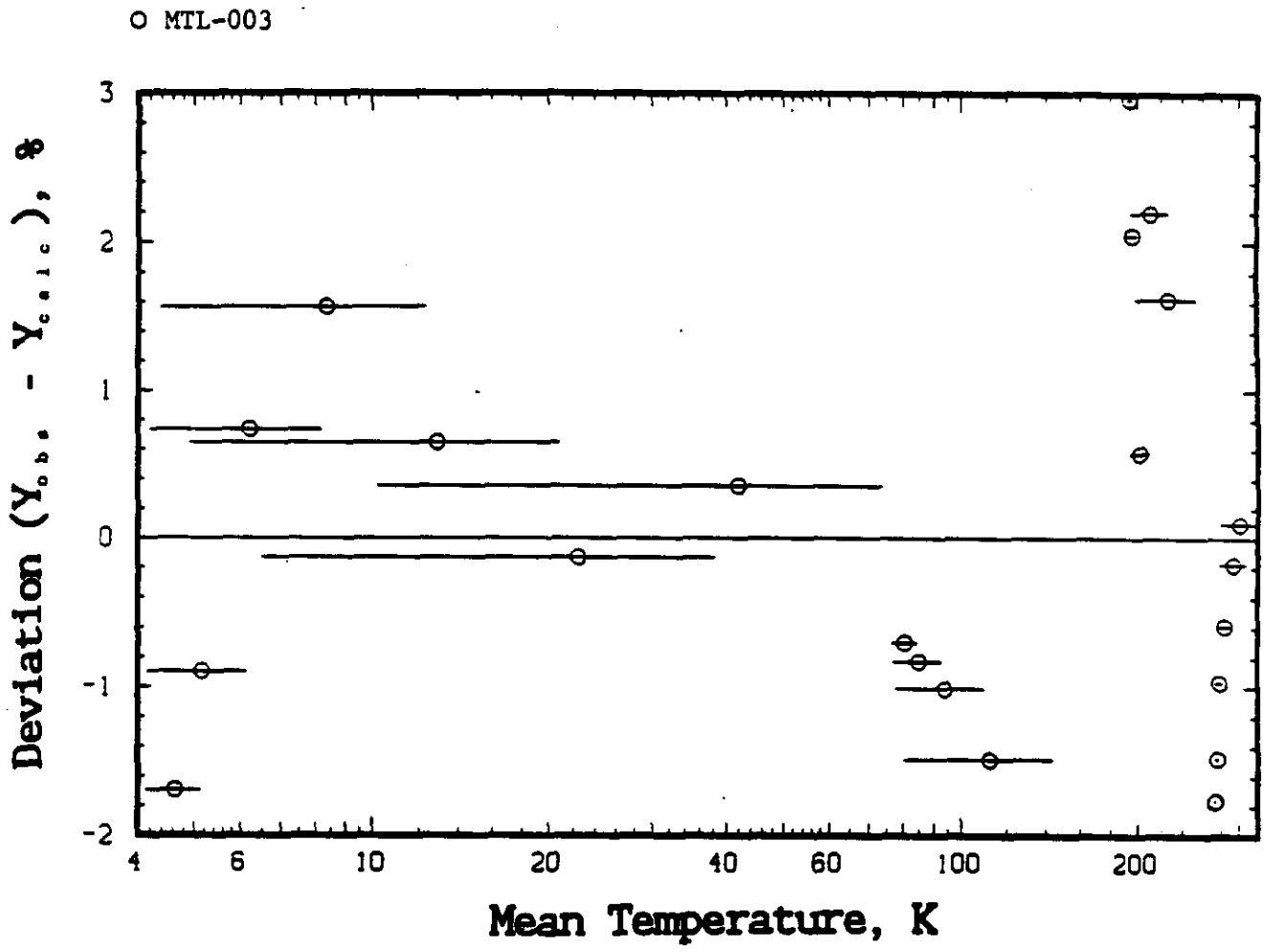

Figure 13. Relative deviations of experimental and calculated thermal conductivity integrals for PPMI film specimen MTL-003. The horizontal bar indicates the span of temperature for each run.

Table 12. Experimental conductivity as a function of temperature for PPMI film MT-003.

ΔT Setting	Average Temperature Kelvin	Thermal Conductivity W/(m·K)	Cold Bath
1	4.629	0.010	LHe
2	5.139	0.012	
4	6.177	0.015	
8	8.274	0.024	
16	12.615	0.042	
16	12.623	0.043	
32	21.808	0.082	
64	40.800	0.154	
4	78.157	0.263	LN_2
8	80.316	0.265	
16	84.657	0.275	
24	89.054	0.286	
24	89.091	0.285	
32	93.407	0.293	
64	111.128	0.323	
4	194.341	0.441	CO_2-alcohol
8	196.690	0.444	
16	201.402	0.446	
64	230.188	0.457	
1	273.736	0.484	Ice-water
2	274.323	0.485	
4	275.499	0.488	
8	277.853	0.489	
16	282.586	0.494	
32	292.133	0.500	
54	305.489	0.511	

Table 13. Experimental conductivity as a function of temperature for PPMI film MT-003-R (retest).

ΔT Setting	Average Temperature Kelvin	Thermal Conductivity W/(m·K)	Cold Bath
1	4.629	0.011	LHe
8	8.274	0.025	
32	21.824	0.084	
65	41.389	0.157	
32	93.390	0.293	LN_2
64	111.074	0.321	
1	192.587	0.464	CO_2-alcohol
32	210.857	0.448	
64	230.116	0.456	
1	273.736	0.485	Ice-water
8	277.848	0.491	
32	292.120	0.504	
55	306.082	0.513	

Table 14. Thermal conductivity values as a function of temperature for specimen PPMI film MT-003.

T K	λ(T) W/(m·K)	T K	λ(T) W/(m·K)	T K	λ(T) W/(m·K)	T K	λ(T) W/(m·K)
4.10	0.010	9.10	0.026	51.00	0.193	110.00	0.326
4.20	0.010	9.20	0.026	52.00	0.196	120.00	0.342
4.30	0.010	9.30	0.027	53.00	0.199	130.00	0.357
4.40	0.010	9.40	0.027	54.00	0.202	140.00	0.371
4.50	0.011	9.50	0.028	55.00	0.205	150.00	0.384
4.60	0.011	9.60	0.028	56.00	0.208	160.00	0.396
4.70	0.011	9.70	0.029	57.00	0.211	170.00	0.407
4.80	0.011	9.80	0.029	58.00	0.214	180.00	0.418
4.90	0.011	9.90	0.029	59.00	0.216	190.00	0.428
5.00	0.012	10.00	0.030	60.00	0.219	200.00	0.437
5.10	0.012	11.00	0.034	61.00	0.222	210.00	0.446
5.20	0.012	12.00	0.039	62.00	0.225	220.00	0.454
5.30	0.012	13.00	0.044	63.00	0.227	230.00	0.462
5.40	0.013	14.00	0.049	64.00	0.230	240.00	0.469
5.50	0.013	15.00	0.053	65.00	0.232	250.00	0.477
5.60	0.013	16.00	0.058	66.00	0.235	260.00	0.483
5.70	0.013	17.00	0.063	67.00	0.238	270.00	0.490
5.80	0.014	18.00	0.067	68.00	0.240	280.00	0.496
5.90	0.014	19.00	0.072	69.00	0.243	290.00	0.502
6.00	0.014	20.00	0.077	70.00	0.245	300.00	0.507
6.10	0.015	21.00	0.081	71.00	0.247	310.00	0.512
6.20	0.015	22.00	0.086	72.00	0.250	320.00	0.517
6.30	0.015	23.00	0.090	73.00	0.252	330.00	0.522
6.40	0.015	24.00	0.095	74.00	0.255		
6.50	0.016	25.00	0.099	75.00	0.257		
6.60	0.016	26.00	0.103	76.00	0.259		
6.70	0.017	27.00	0.107	77.00	0.261		
6.80	0.017	28.00	0.112	78.00	0.264		
6.90	0.017	29.00	0.116	79.00	0.266		
7.00	0.018	30.00	0.120	80.00	0.268		
7.10	0.018	31.00	0.124	81.00	0.270		
7.20	0.018	32.00	0.128	82.00	0.273		
7.30	0.019	33.00	0.132	83.00	0.275		
7.40	0.019	34.00	0.135	84.00	0.277		
7.50	0.019	35.00	0.139	85.00	0.279		
7.60	0.020	36.00	0.143	86.00	0.281		
7.70	0.020	37.00	0.147	87.00	0.283		
7.80	0.021	38.00	0.150	88.00	0.285		
7.90	0.021	39.00	0.154	89.00	0.287		
8.00	0.021	40.00	0.157	90.00	0.289		
8.10	0.022	41.00	0.161	91.00	0.291		
8.20	0.022	42.00	0.164	92.00	0.293		
8.30	0.023	43.00	0.168	93.00	0.295		
8.40	0.023	44.00	0.171	94.00	0.297		
8.50	0.023	45.00	0.174	95.00	0.299		
8.60	0.024	46.00	0.178	96.00	0.301		
8.70	0.024	47.00	0.181	97.00	0.303		
8.80	0.025	48.00	0.184	98.00	0.305		
8.90	0.025	49.00	0.187	99.00	0.307		
9.00	0.026	50.00	0.190	100.00	0.308		

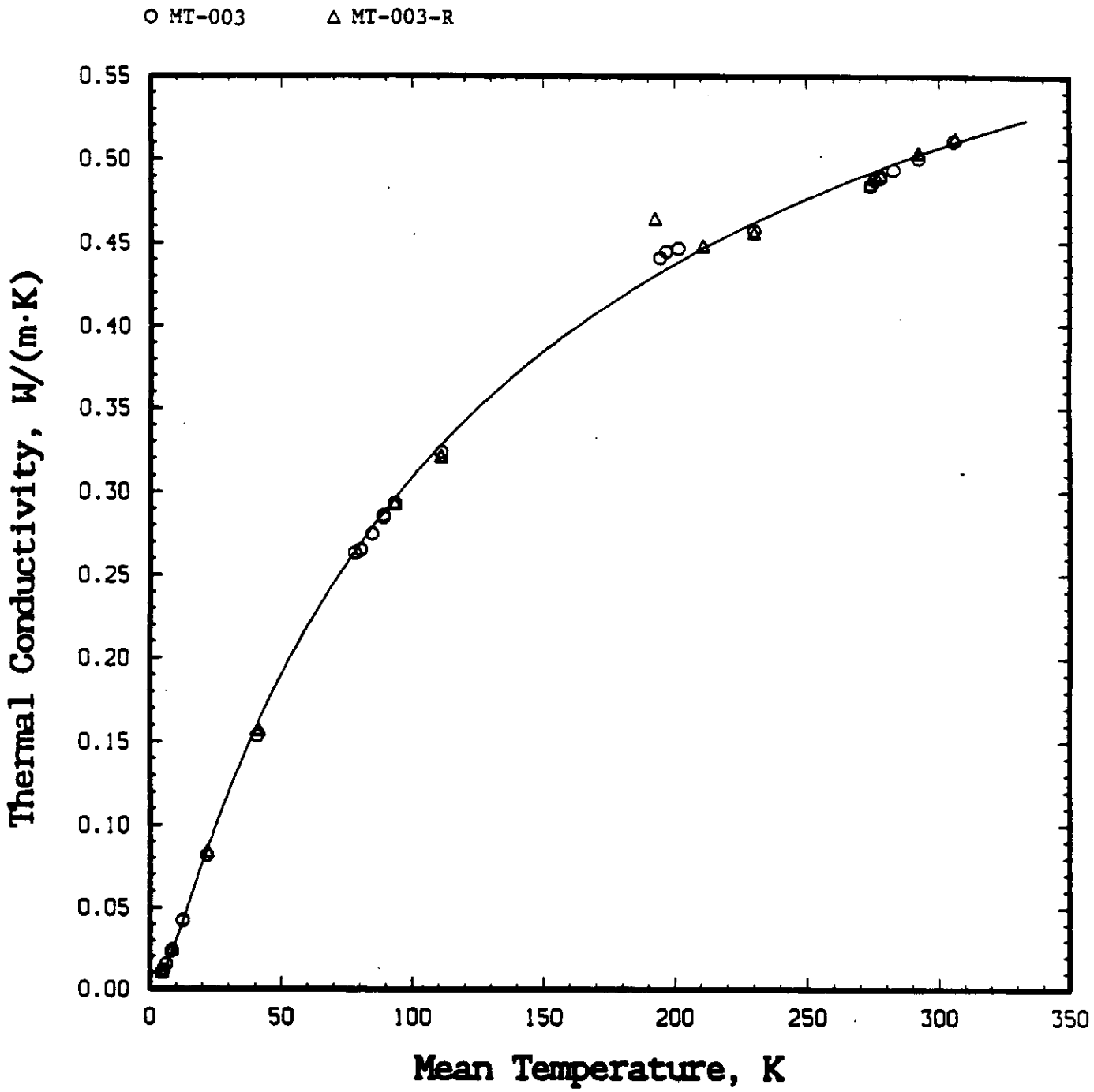

Figure 14. Thermal conductivity of PPMI film specimen MT-003 and MT-003-R (repeated measurements on same specimen). Experimental data are presented as discrete points. Two specimens were tested to determine reproducibility. Both scales are linear, which clarifies the behavior at high temperatures.

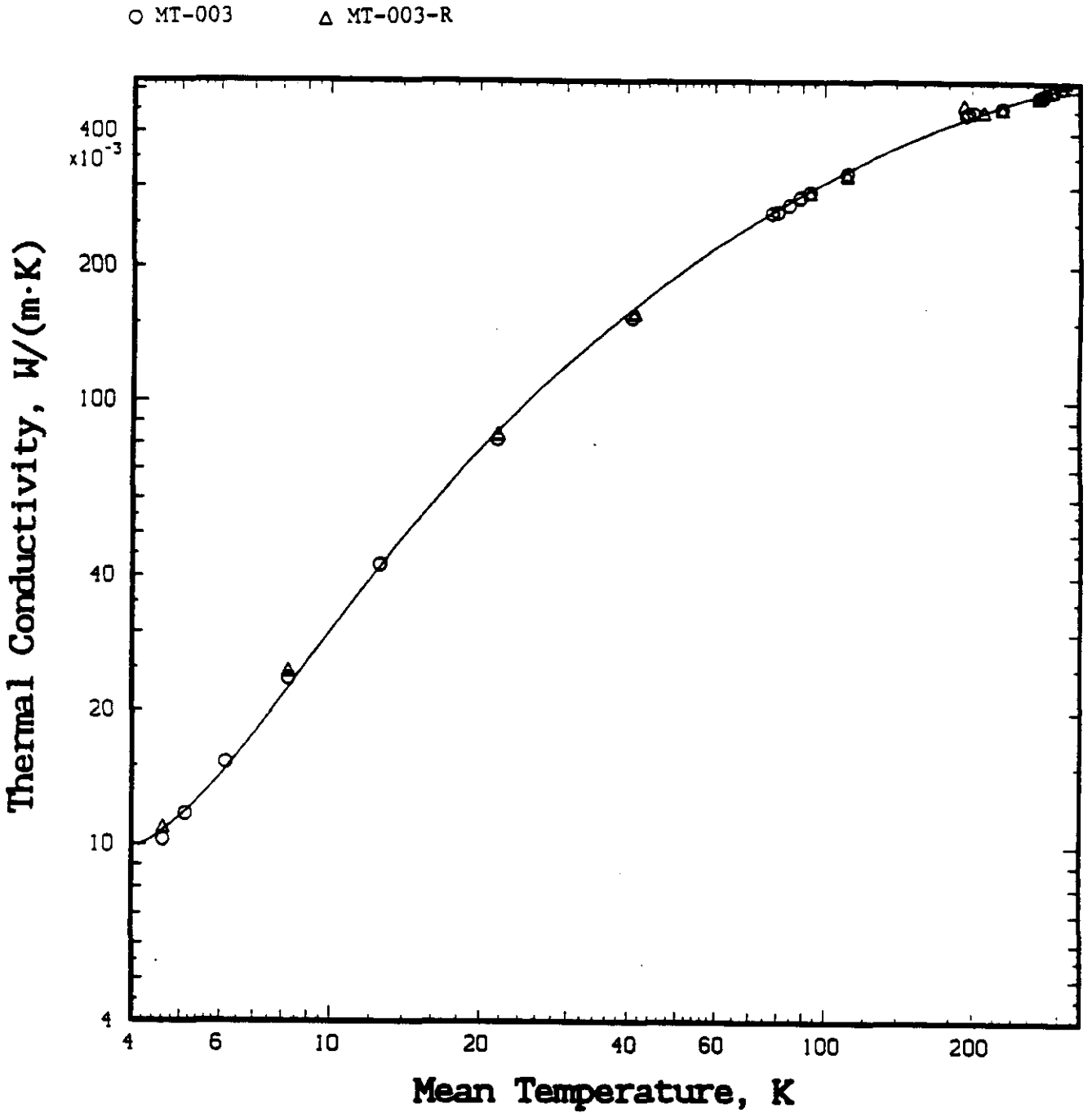

Figure 15. Thermal conductivity of PPMI film specimen MT-003 and MT-003-R (repeated measurements on same specimen). Experimental data are presented as discrete points. Two specimens were tested to determine reproducibility. Both scales are logarithmic, which clarifies the behavior at low temperatures.

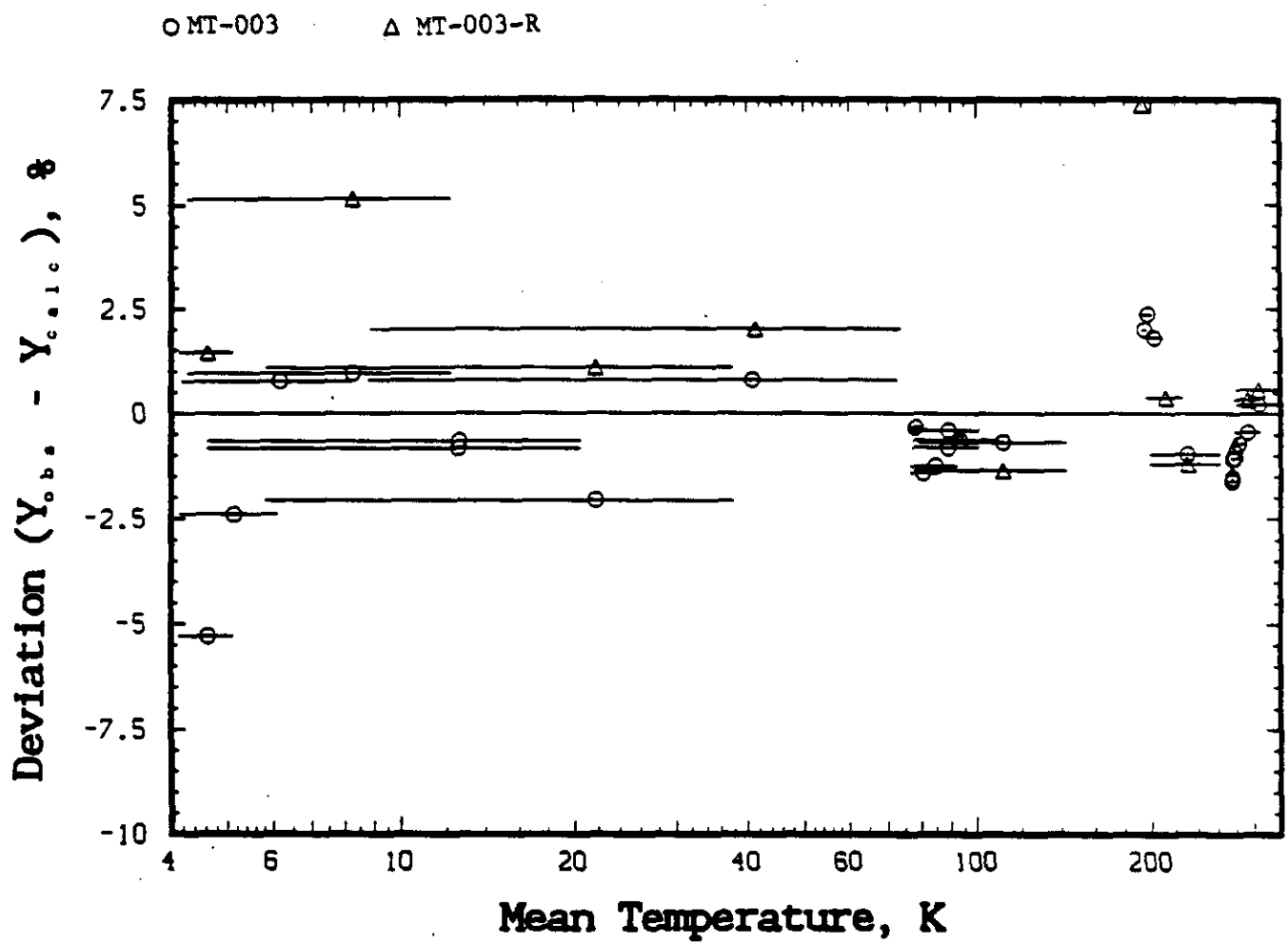

Figure 16. Relative deviations of experimental and calculated thermal conductivity integrals for PPMI film specimen MT-003 and MT-003-R (repeated measurements on same specimen). The horizontal bar indicates the span of temperature used for each run.

Table 15. Experimental conductivity as a function of temperature for PPMI film MT-001.

ΔT Setting	Average Temperature Kelvin	Thermal Conductivity W/(m·K)	Cold Bath
2	5.142	0.014	LHe
4	6.181	0.018	
8	8.282	0.027	
16	12.656	0.047	
32	21.839	0.086	
64	40.784	0.157	
16	84.656	0.282	LN_2
32	93.398	0.300	
32	93.398	0.300	
64	111.107	0.330	
64	111.110	0.330	
1	192.584	0.451	CO_2-alcohol
8	196.678	0.449	
16	201.378	0.449	
32	210.906	0.465	
64	230.135	0.464	
1	273.736	0.494	Ice-water
2	274.323	0.497	
4	275.497	0.497	
8	277.850	0.500	
16	282.577	0.503	
32	292.119	0.511	
54.5	305.737	0.522	

Table 16. Thermal conductivity values as a function of temperature for specimen PPMI film MT-001.

T, K	λ(T), W/(m·K)	T, K	λ(T), W/(m·K)	T, K	λ(T), W/(m·K)	T K	λ(T) W/(m·K)
4.10	0.013	9.10	0.029	51.00	0.198	110.00	0.333
4.20	0.013	9.20	0.029	52.00	0.201	120.00	0.349
4.30	0.013	9.30	0.030	53.00	0.204	130.00	0.364
4.40	0.013	9.40	0.030	54.00	0.207	140.00	0.378
4.50	0.013	9.50	0.031	55.00	0.210	150.00	0.391
4.60	0.014	9.60	0.031	56.00	0.213	160.00	0.403
4.70	0.014	9.70	0.032	57.00	0.216	170.00	0.415
4.80	0.014	9.80	0.032	58.00	0.219	180.00	0.426
4.90	0.014	9.90	0.032	59.00	0.222	190.00	0.436
5.00	0.014	10.00	0.033	60.00	0.224	200.00	0.445
5.10	0.015	11.00	0.037	61.00	0.227	210.00	0.454
5.20	0.015	12.00	0.042	62.00	0.230	220.00	0.462
5.30	0.015	13.00	0.047	63.00	0.232	230.00	0.470
5.40	0.015	14.00	0.052	64.00	0.235	240.00	0.478
5.50	0.016	15.00	0.056	65.00	0.238	250.00	0.485
5.60	0.016	16.00	0.061	66.00	0.240	260.00	0.492
5.70	0.016	17.00	0.066	67.00	0.243	270.00	0.498
5.80	0.017	18.00	0.071	68.00	0.245	280.00	0.505
5.90	0.017	19.00	0.075	69.00	0.248	290.00	0.510
6.00	0.017	20.00	0.080	70.00	0.250	300.00	0.516
6.10	0.017	21.00	0.085	71.00	0.253	310.00	0.521
6.20	0.018	22.00	0.089	72.00	0.255	320.00	0.526
6.30	0.018	23.00	0.094	73.00	0.258	330.00	0.531
6.40	0.018	24.00	0.098	74.00	0.260		
6.50	0.019	25.00	0.103	75.00	0.263		
6.60	0.019	26.00	0.107	76.00	0.265		
6.70	0.019	27.00	0.111	77.00	0.267		
6.80	0.020	28.00	0.115	78.00	0.269		
6.90	0.020	29.00	0.120	79.00	0.272		
7.00	0.021	30.00	0.124	80.00	0.274		
7.10	0.021	31.00	0.128	81.00	0.276		
7.20	0.021	32.00	0.132	82.00	0.278		
7.30	0.022	33.00	0.136	83.00	0.281		
7.40	0.022	34.00	0.139	84.00	0.283		
7.50	0.022	35.00	0.143	85.00	0.285		
7.60	0.023	36.00	0.147	86.00	0.287		
7.70	0.023	37.00	0.151	87.00	0.289		
7.80	0.024	38.00	0.154	88.00	0.291		
7.90	0.024	39.00	0.158	89.00	0.293		
8.00	0.024	40.00	0.162	90.00	0.295		
8.10	0.025	41.00	0.165	91.00	0.297		
8.20	0.025	42.00	0.169	92.00	0.299		
8.30	0.026	43.00	0.172	93.00	0.301		
8.40	0.026	44.00	0.175	94.00	0.303		
8.50	0.026	45.00	0.179	95.00	0.305		
8.60	0.027	46.00	0.182	96.00	0.307		
8.70	0.027	47.00	0.185	97.00	0.309		
8.80	0.028	48.00	0.189	98.00	0.311		
8.90	0.028	49.00	0.192	99.00	0.313		
9.00	0.029	50.00	0.195	100.00	0.315		

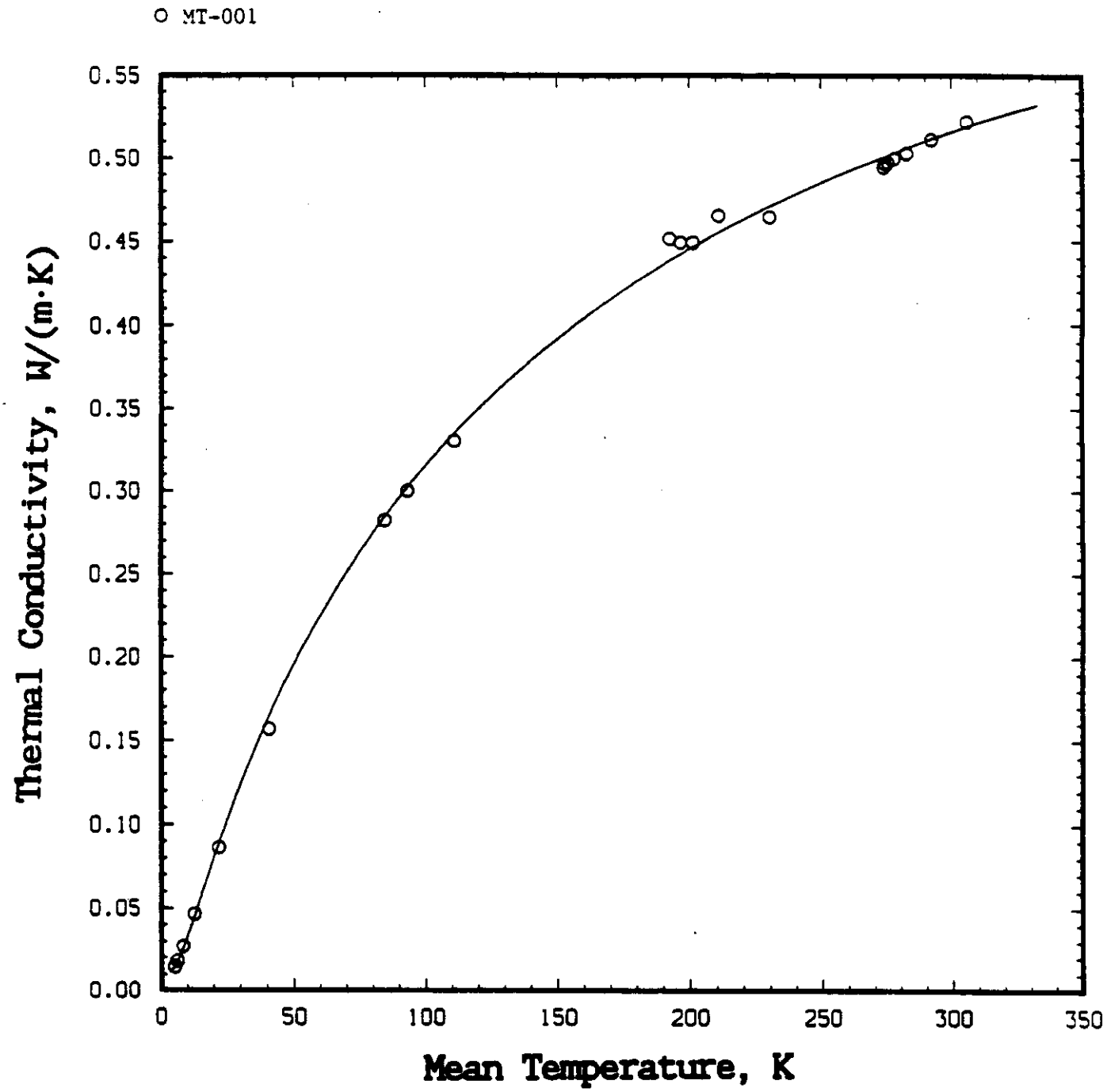

Figure 17. Thermal conductivity of PPMI film specimen MT-001. Experimental data are presented as discrete points. Both scales are linear, which clarifies the behavior at high temperatures.

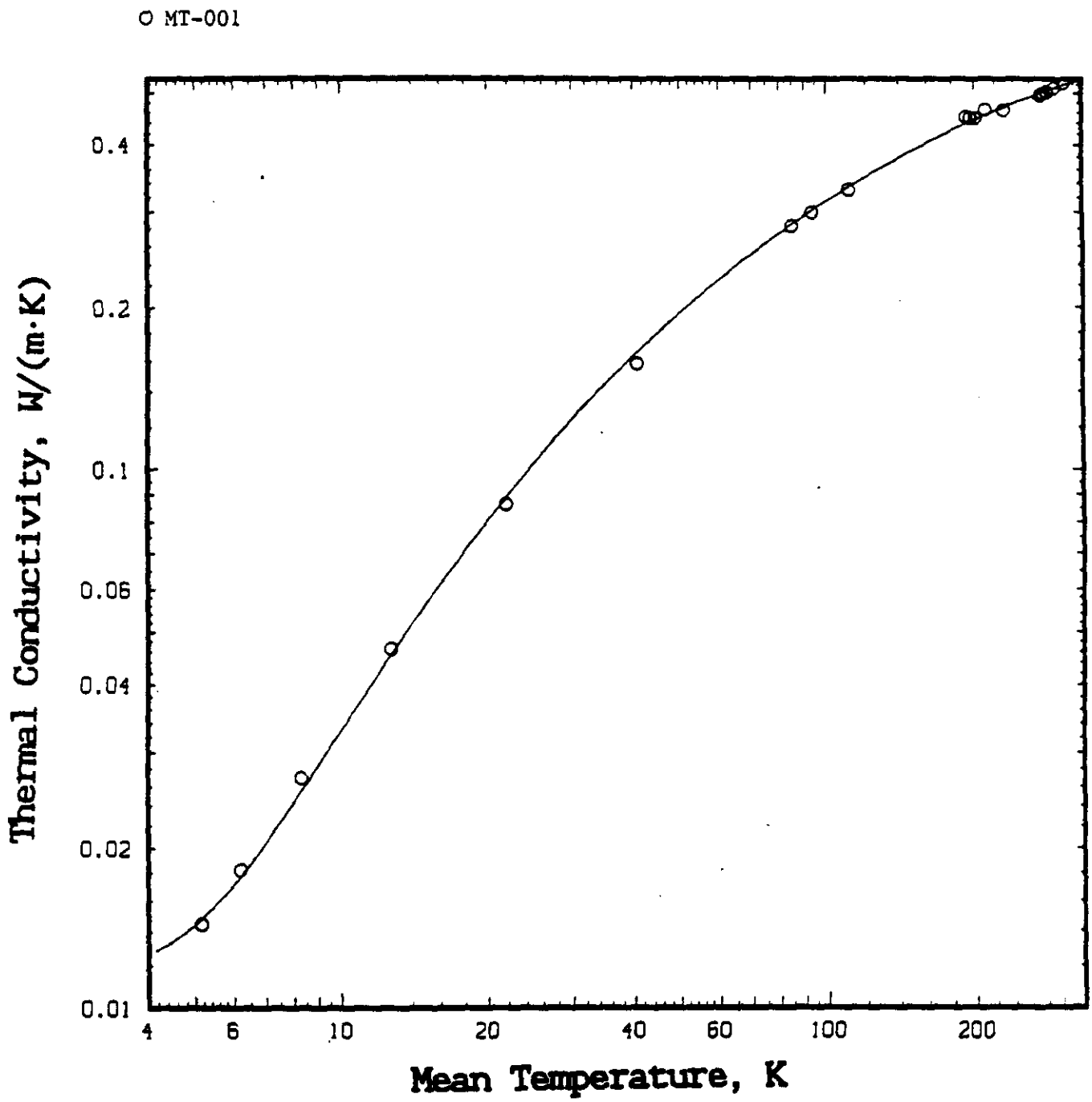

Figure 18. Thermal conductivity of PPMI film specimen MT-001. Experimental data are presented as discrete points. Both scales are logarithmic, which clarifies the behavior at low temperatures.

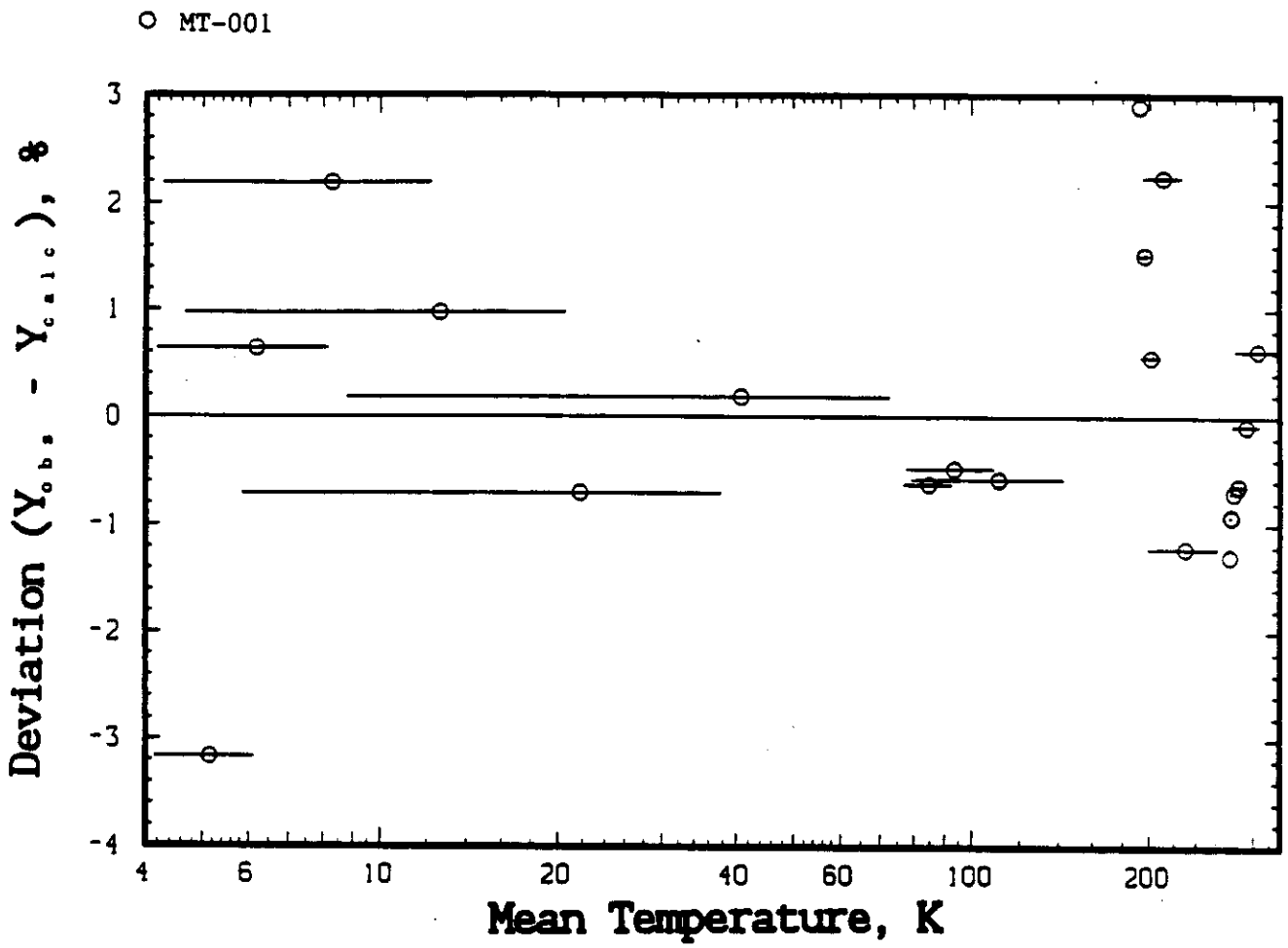

Figure 19. Relative deviations of experimental and calculated thermal conductivity integrals for PPMI film specimen MT-001. The horizontal bar indicates the span of temperature for each run.

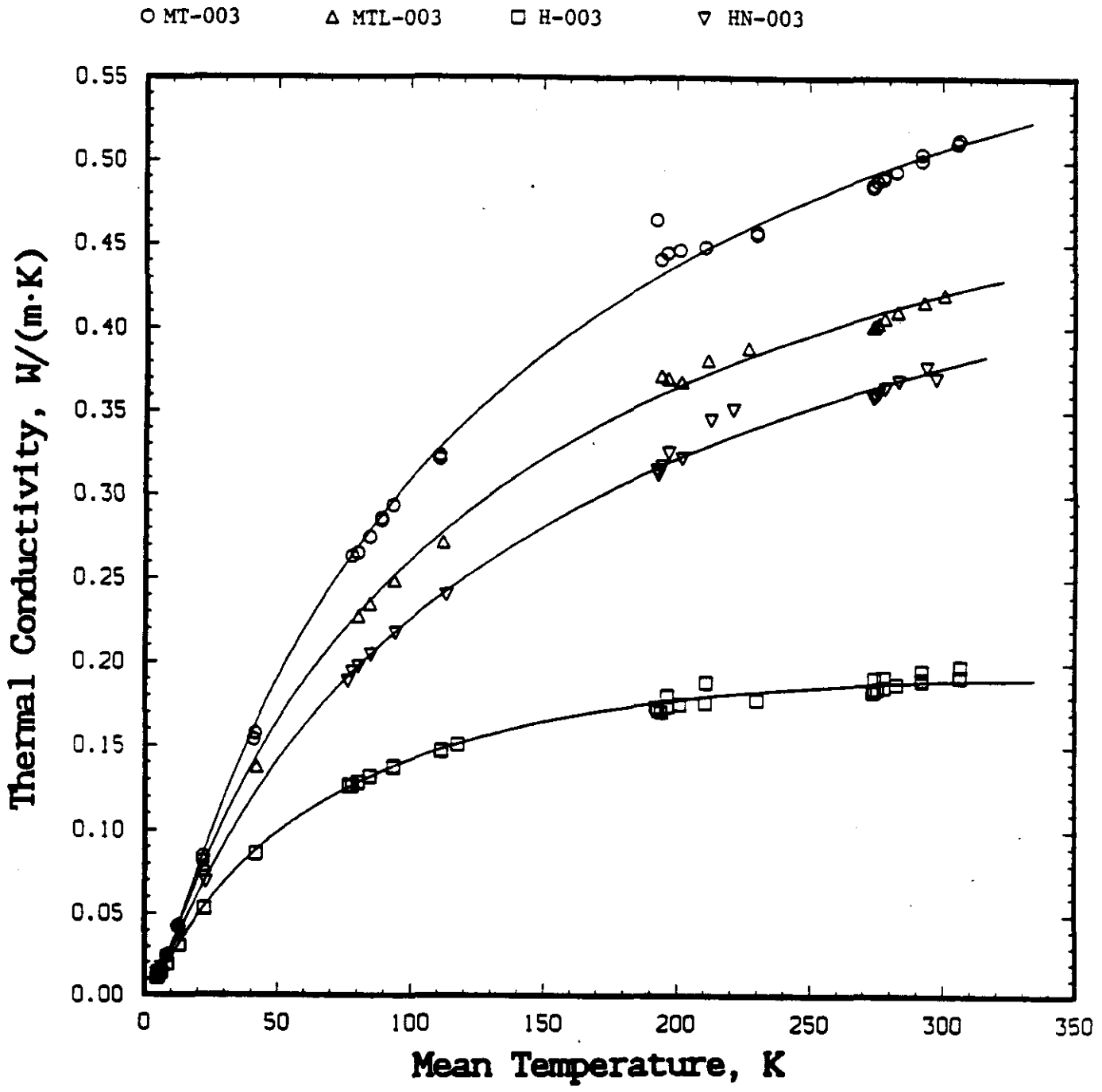

Figure 20. Thermal conductivity of four PPMI film specimens composed of layers of film 76 μm thick. Experimental data are presented as discrete points. [[Specimens MT-003 and H-003 were retested to determine reproducibility.]] Both scales are linear, which clarifies the behavior at high temperatures.

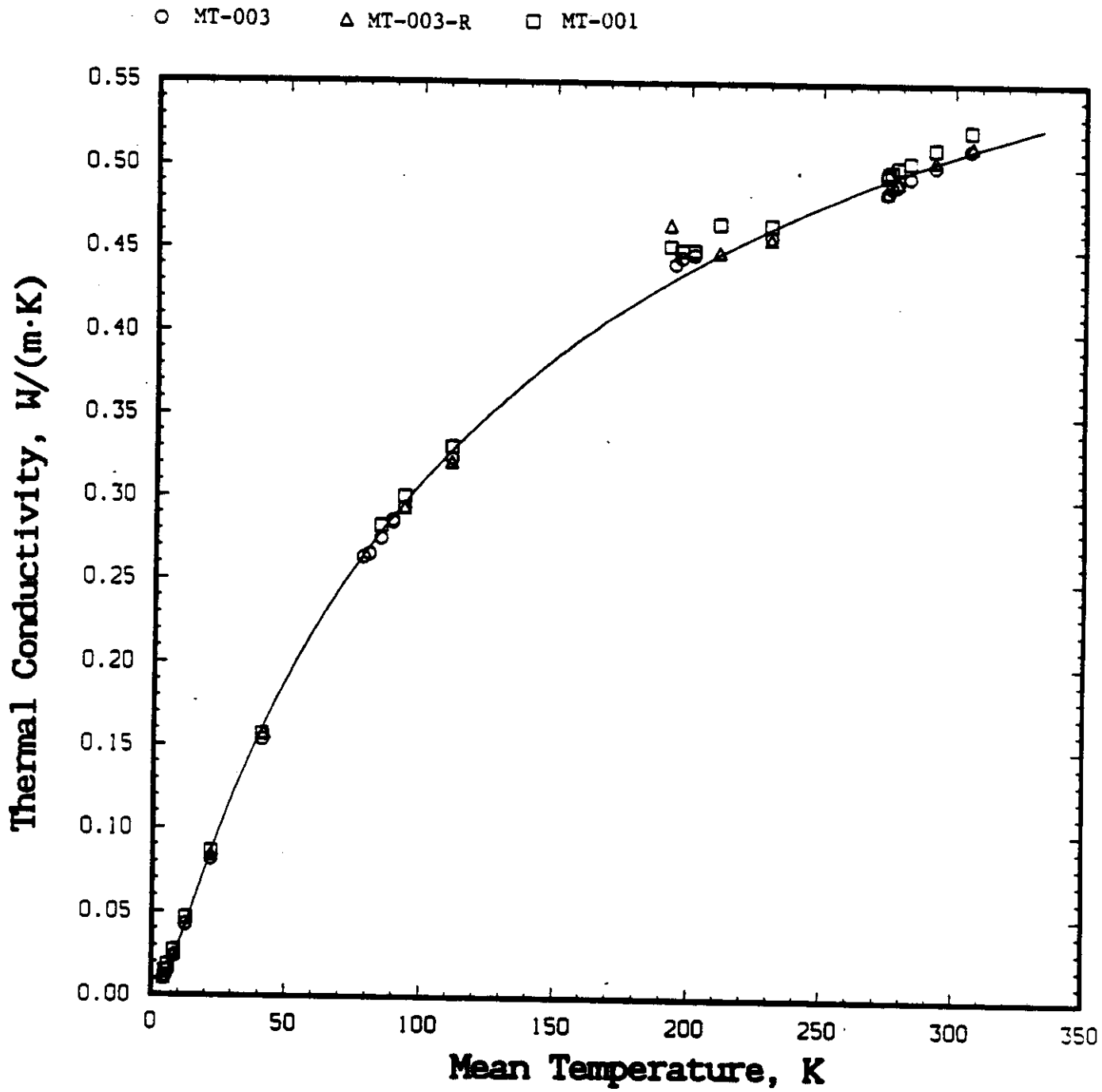

Figure 22. Intercomparison of thermal conductivity of PPMI film specimens MT-003 (thickness: 76 μm) and MT-001 (thickness: 25 μm).

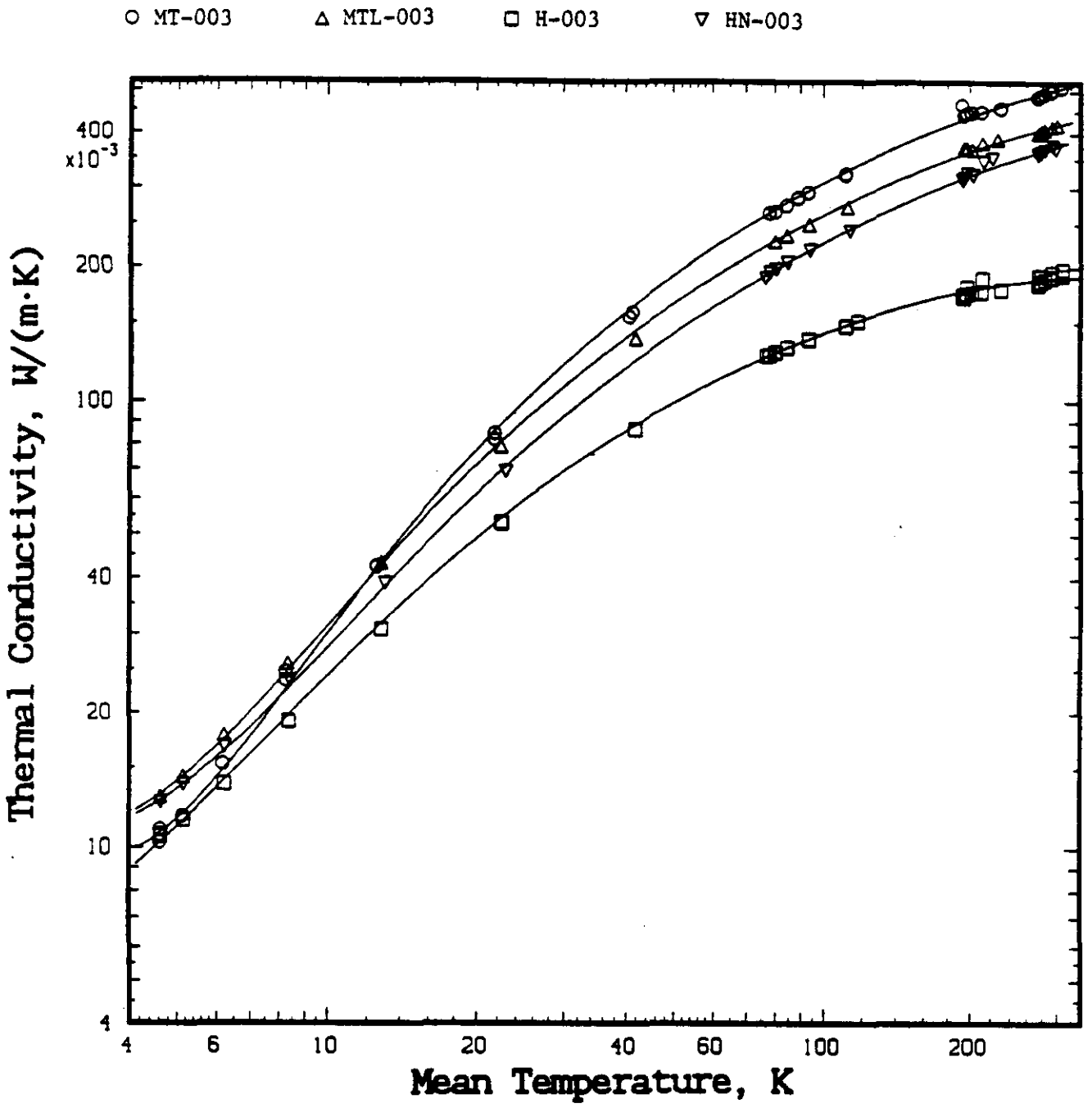

Figure 21. Thermal conductivity of four PPMI film specimens composed of layers of film 76 μm thick. Experimental data are presented as discrete points. Both scales are logarithmic, which clarifies the behavior at low temperatures.

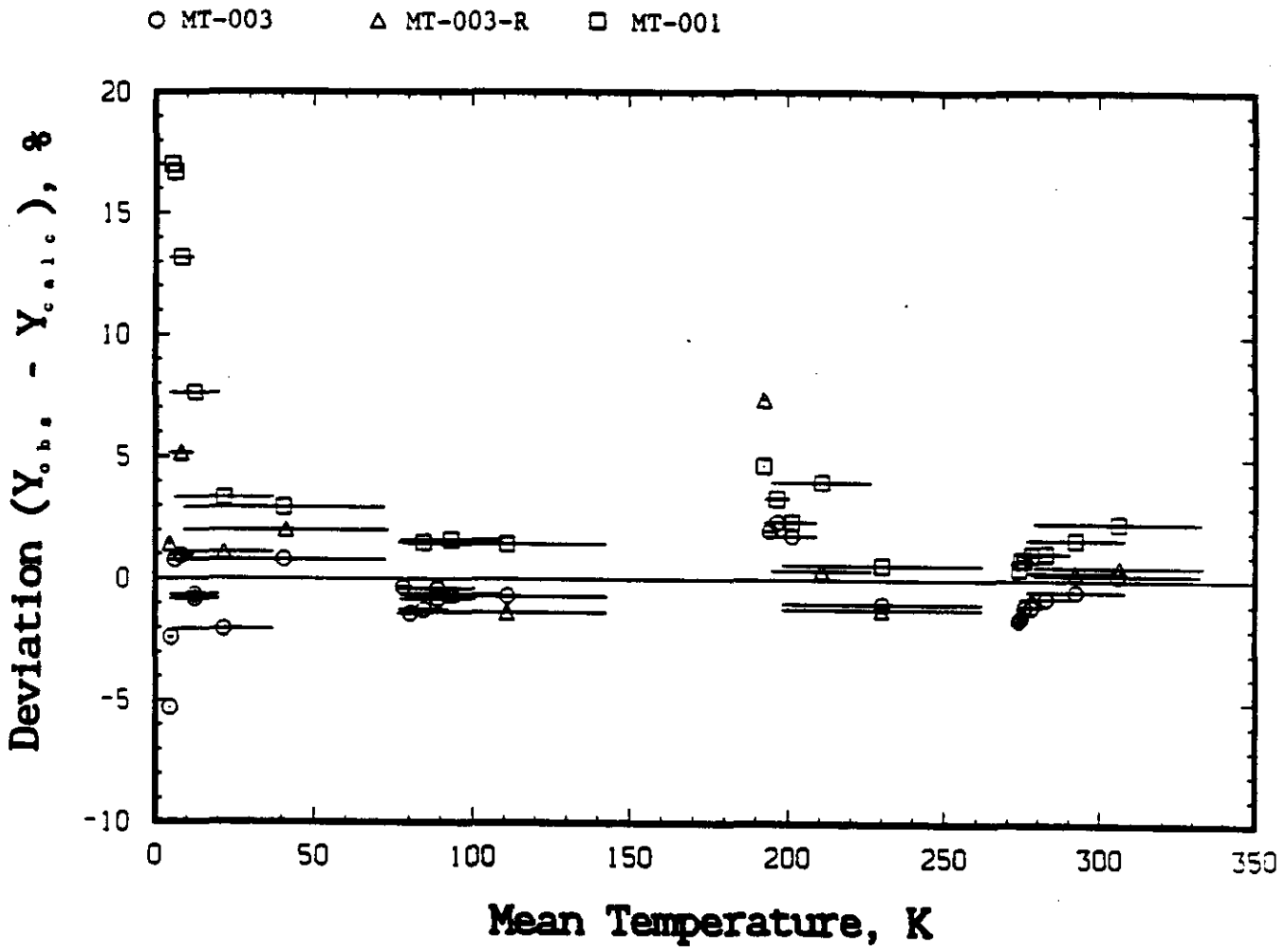

Figure 23. Comparison of relative deviation of experimental data (open squares) for PPMI film specimen MT-001 (25 μm) with both calculated thermal conductivity (fitted curve) and experimental data (open circles and triangles) for film specimen MT-003 (76 μm).

Table 17. Experimental conductivity and ΔT/Q per layer of film as a function of applied mechanical pressure.

Pressure, MPa	Calculated ΔT/Q per layer of film K/w	Apparent Thermal Conductivity, W/(m·K)	Cold Bath
4.8	0.562	0.456	Ice-water
4.8	0.564	0.455	
7.2	0.545	0.470	
7.2	0.545	0.470	
12	0.521	0.492	
14	0.519	0.494	
17	0.525	0.488	
17	0.525	0.488	
4.8	1.060	0.242	LN
7.2	0.998	0.257	
7.2	0.999	0.256	
12	0.945	0.271	
14	0.938	0.273	
14	0.936	0.274	
17	0.943	0.272	
17	0.945	0.271	
4.8	11.37	0.022	LHe
7.2	11.25	0.023	
7.2	11.28	0.023	
12	10.33	0.025	
14	9.79	0.026	
14	10.00	0.026	
17	10.44	0.024	

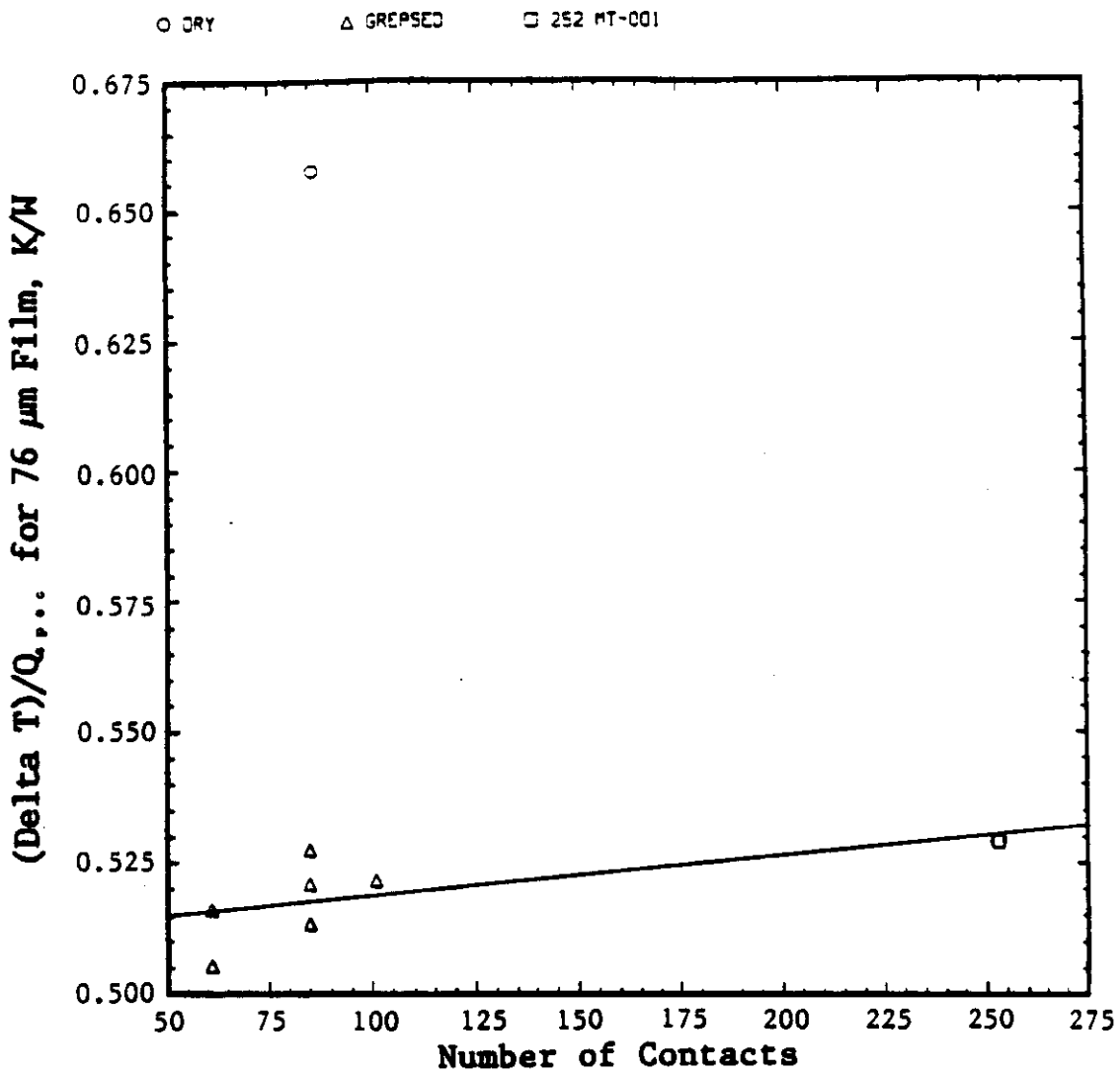

Figure 24. Thermal contact resistance, ΔT/Q, per layer of PPMI film, at a mean specimen temperature of 277.5 K, as a function of number of interfacial contacts. Open triangles and squares represent specimens composed of greased interfaces, and the open circle is for one specimen of ungreased (dry) interfaces, for 76-μm (MT-003: 0.003 in) PPMI film. The open square represents thermal resistance for 252 layers of 25-μm (MT-001: 0.001 in) film; the value has been scaled by a factor of 3 to give the equivalent resistance per layer of 84 (252/3) layers 0.003 in thick. The resistance per layer for the values for MT-003 and the scaled value for the much larger number of layers of MT-001 agree within experimental uncertainty. This shows the absence of any measurable dependence of conductivity on thickness, and that contact resistance for greased interfaces is negligible. The straight line is a least-squares fit to the points for greased interfaces. The open circle at 84 layers, 0.66 K/W, lies 0.14 K/W (27 percent) higher than the line; the difference represents the contact resistance of the interface between two adjacent dry films.

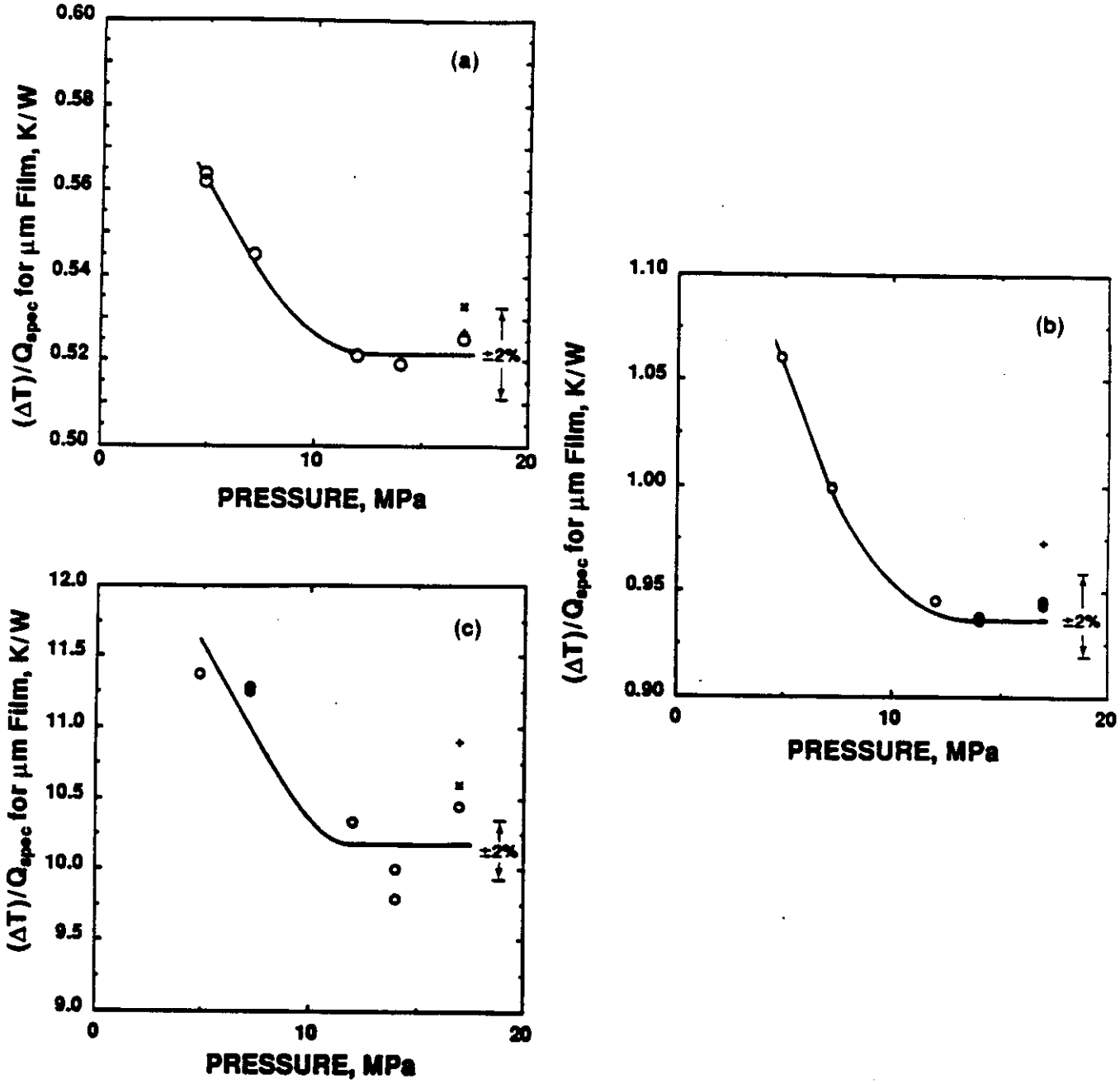

Figure 25. Thermal contact resistance, ΔT/Q, per layer of 76-µm PPMI film (specimen MT-003-P), as a function of mechanical pressure, at mean specimen temperatures of (a) 277.8 K (ice), (b) 80.3 K (LN_2), and (c) 8.3 K (LHe). Data points "+" in each plot represent contact resistance for a different specimen (MT-003) of the same material under the same conditions, calculated from table 12. Points "X" represent contact resistance for specimen MT-003-R of the same material under the same conditions, calculated from data in table 13. Error bars for each curve provide scales with which to judge the amount of scatter in the data. At all measurement temperatures, experimental reproducibility (imprecision) is within about 2 percent. Within this imprecision, contact resistance appears to become independent of pressure, for pressures above about 12 MPa (1.7 kpsi), at all three mean temperatures.

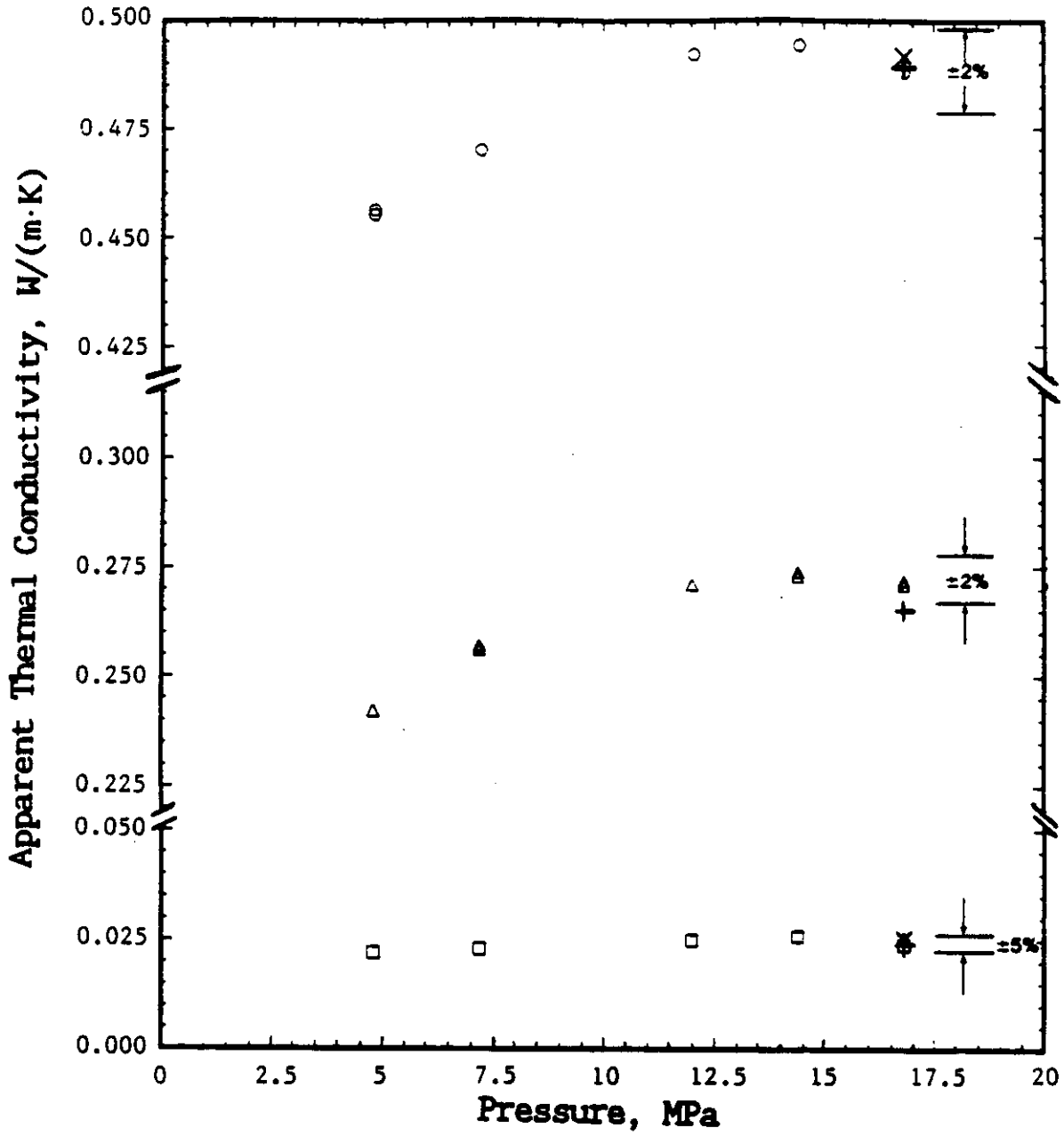

Figure 26. Thermal conductivity as a function of mechanical pressure, corresponding to the data for thermal contact resistance shown in figure 24. Mean specimen temperatures are: (a) open circles: 277.8 K (ice); (b) triangles: 80.3 K (LN); (c) open squares: 8.3 K (LHe). Refer to the caption for figure 25 for the explanation and importance of the error bars. Within experimental imprecision, conductivity appears to become independent of pressure, for pressures above about 12 MPa (1.7 kpsi), at all three mean temperatures.

Table 18. Experimental conductivity as a function of temperature for PPMI film HN-Heat.

ΔT Setting	Average Temperature Kelvin	Thermal Conductivity W/(m·K)	Cold Bath
1	4.640	0.012	LHe
2	5.165	0.013	
4	6.238	0.017	
8	8.435	0.024	
16	13.123	0.039	
32	23.044	0.069	
32	42.859	0.117	
2	77.109	0.196	LN_2
4	78.274	0.198	
16	85.172	0.209	
16	85.181	0.210	
31.7	94.324	0.223	
32	94.496	0.222	
58.2	110.059	0.241	
1	192.638	0.315	CO_2-alcohol
2	193.281	0.319	
8	197.140	0.322	
16	202.337	0.329	
32	212.864	0.338	
52.3	226.339	0.340	
1	273.788	0.370	Ice-water
2	274.425	0.370	
2	274.426	0.370	
4	275.704	0.369	
8	278.267	0.371	
16	283.415	0.373	
32	293.823	0.379	
36	296.450	0.380	

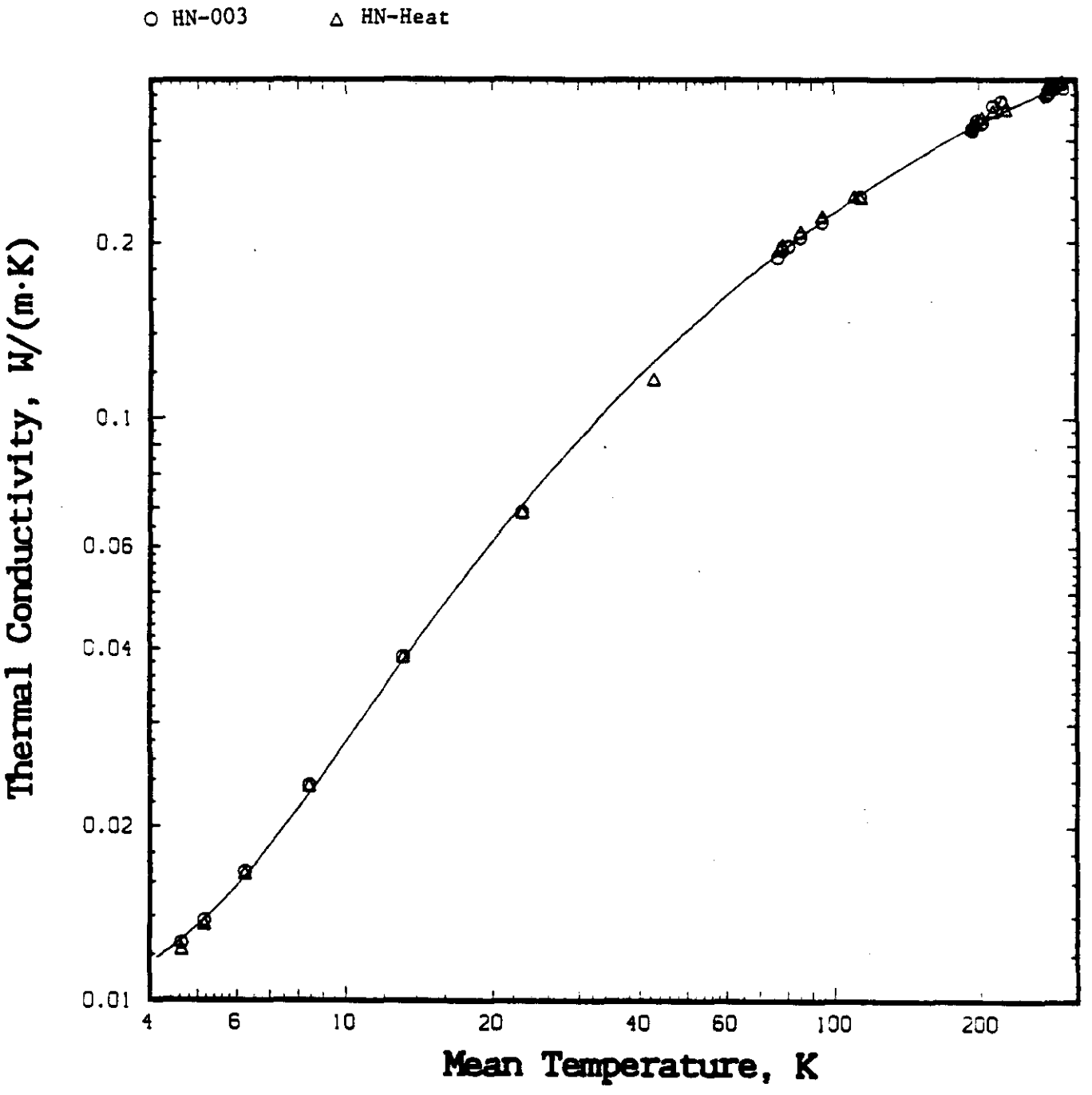

Figure 27. Intercomparison of the thermal conductivity of 76-μm PPMI film before (HN-003) and after (HN-Heat) a heat treatment at 150°C for ninety minutes.

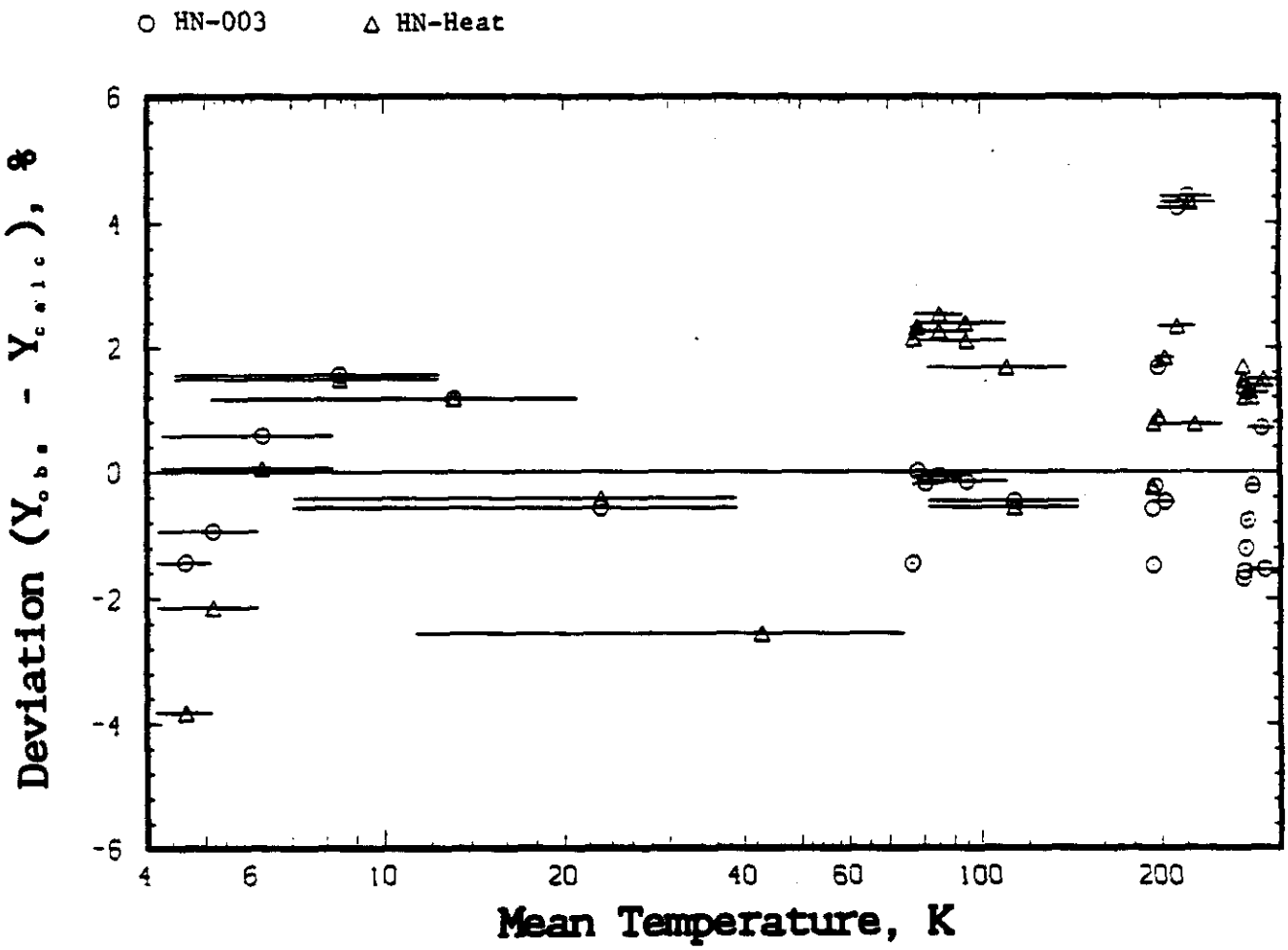

Figure 28. Relative deviations of experimental data for 76-μm PPMI film specimen before (HN-003: open circles) and after (HN-Heat: open triangles) heat treatment, from calculated thermal conductivity (curve fitted to data for HN-003). The similarity in magnitude of deviations shows that the heat treatment had no measurable effect on the thermal conductivity of the film, within experimental imprecision.

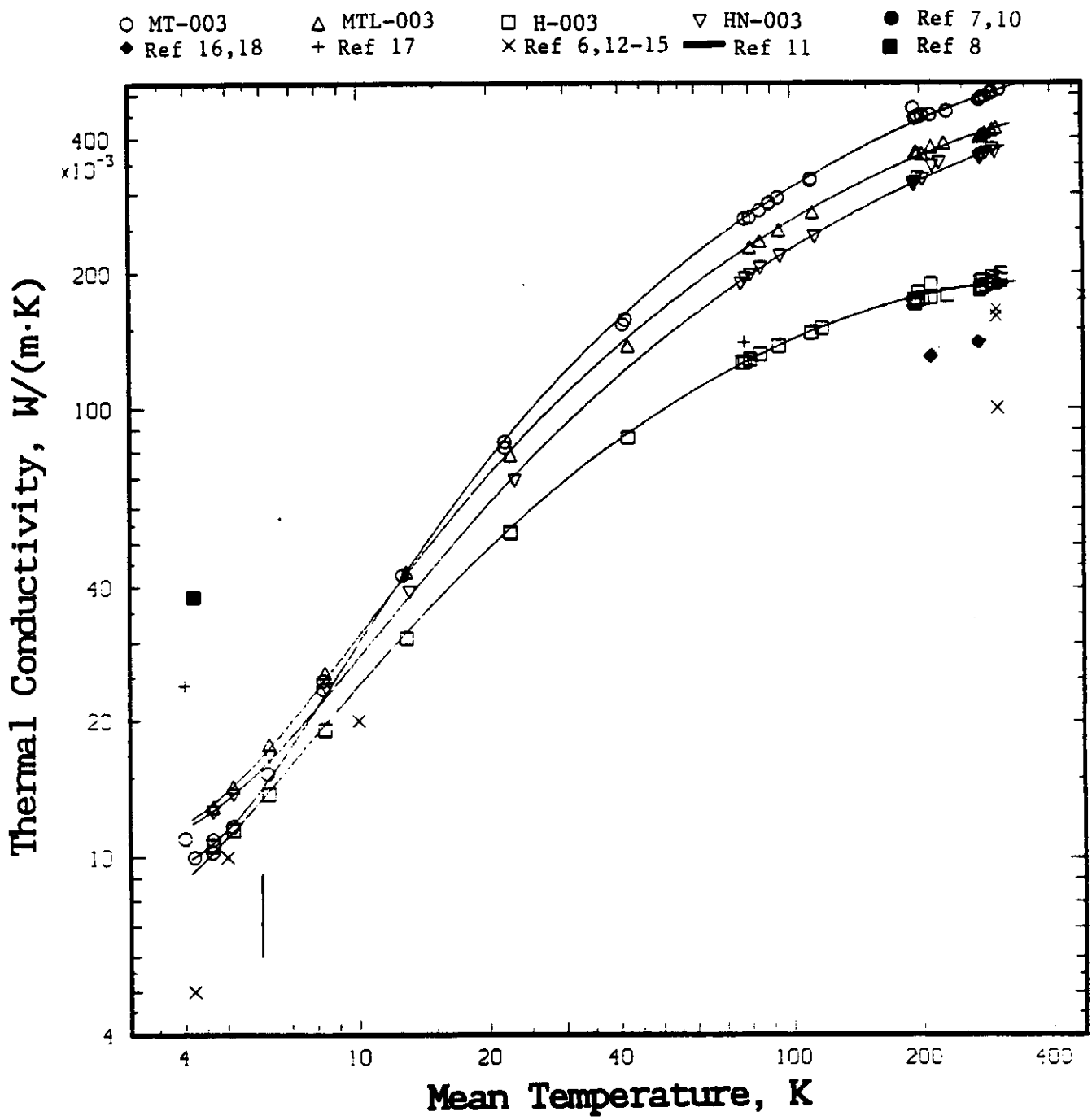

Figure 29. Thermal conductivity of PPMI film specimens composed of layers of film 76 μm thick, as in figure 21. Conductivity data for Kapton or other polyimide films (crosses; Refs. 6, 12-15, 17), Vespel (filled circles; Refs. 7, 10), Kerimid (filled square; Ref. 8), polyethylene (narrow box; Ref. 11), and Mylar (filled triangles; Refs. 16, 18) are also given for intercomparison.

APPENDIX A

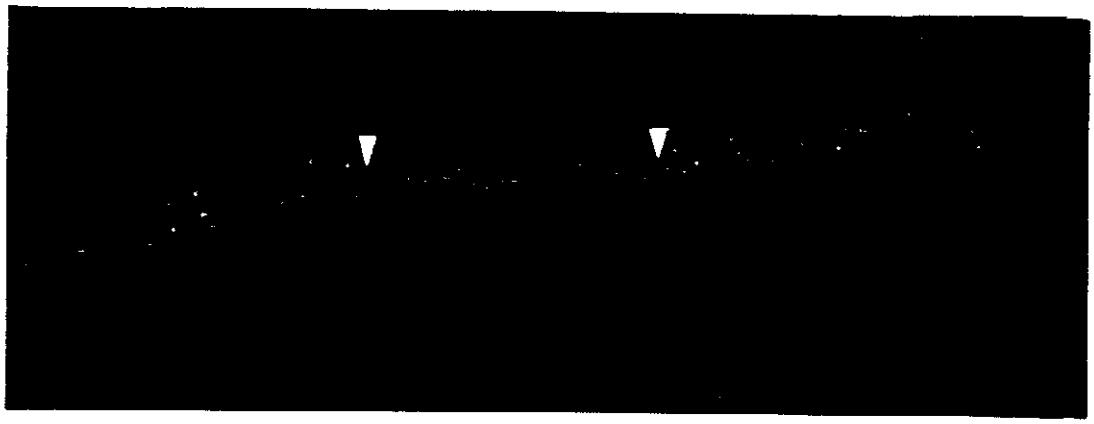

H-003

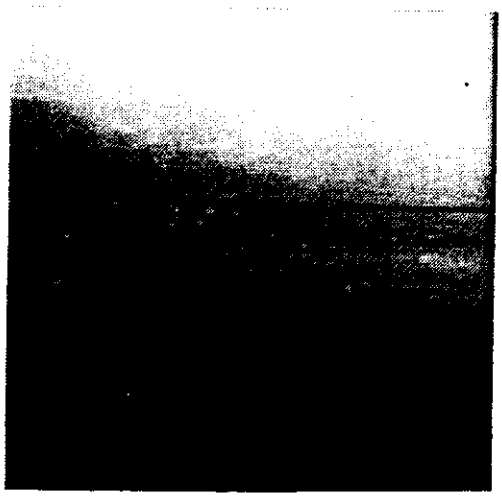

Figure A1. **(Lower)**: Image, from a scanning tunnelling microscope (STM), of a single film of type H unfilled (neat) PPMI (thickness:76 μm) on which a gold layer 30 nm thick was deposited to define the surface. The horizontal line segment bounded by two vertical markers shows the path used to scan the surface roughness.
(Upper): The surface roughness profile along the path parked on the lower STM image, which two triangles marking the portion of the scan corresponding to the segment on the lower image. The grid units are in nanometers. This film specimen was not mounted completely flat, leading to the non-zero slope of the trace from left to right in the image; the surface roughness is approximately 67 nm.

HN-003

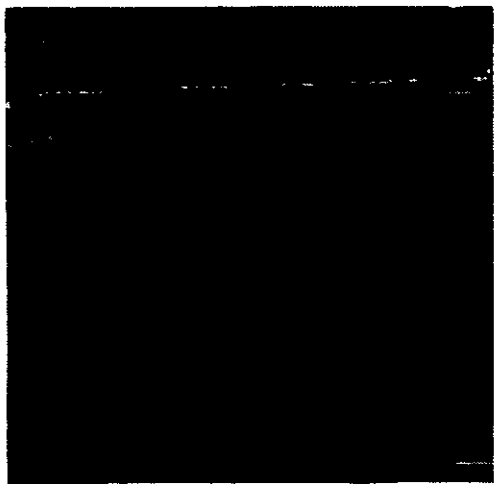

Figure A2. **(Lower)**: STM image of type HN unfilled (neat) PPMI film (thickness: 76 μm) with a 30 nm gold deposition layer.
(Upper): The surface roughness profile for a scan across the surface (grid units: nm). The surface roughness is approximately 32 nm.

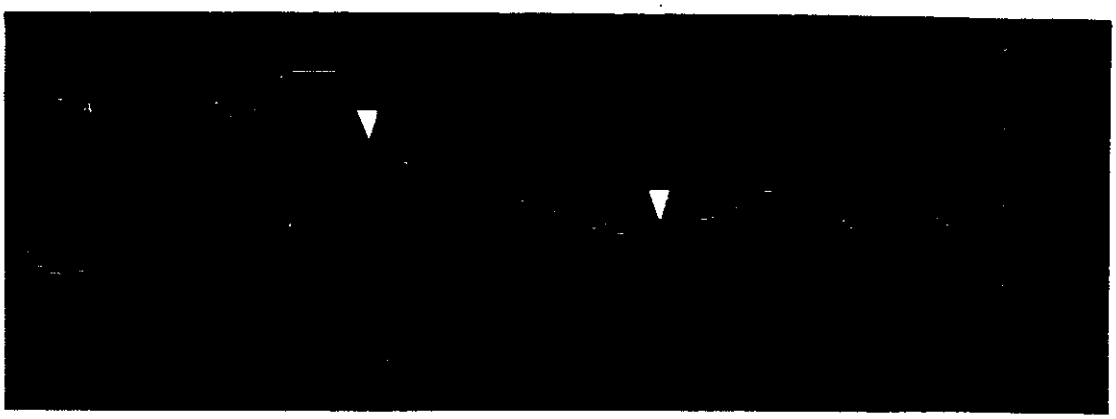

MTL-003

Figure A3. **(Lower)**: STM images of type MTL alumina-filled PPMI film (thickness: 76 μm) with a 30 nm gold deposition layer.
(Upper): The surface roughness profile along the path marked on the lower STM image, with two triangles marking the portion of the scan corresponding to the segment on the lower image. The surface roughness appears to be approximately 250 nm, with some peaks (light regions in the lower image) measuring 1000 nm.

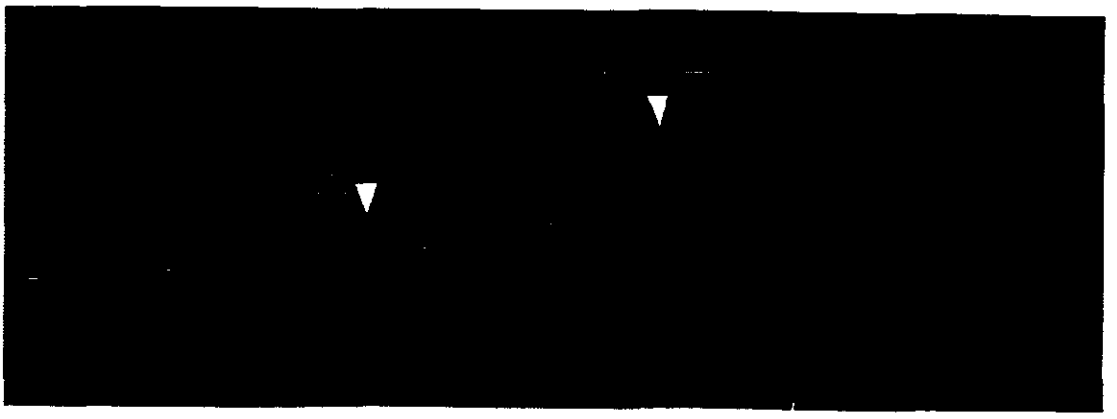

MT-003

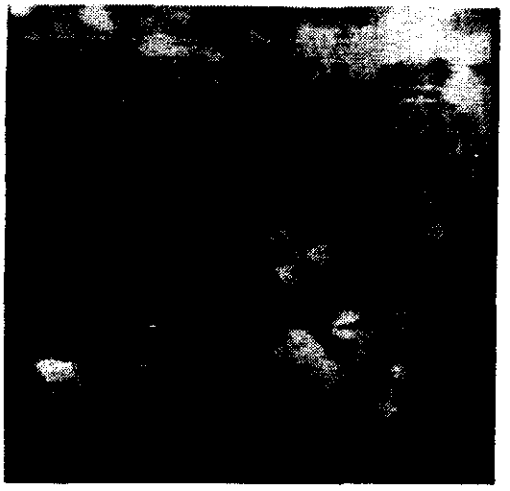

Figure A4. **(Lower)**: STM images of type MT alumina-filled PPMI film (thickness: 76 μm) with a 30 nm gold deposition layer.
(Upper): The surface roughness profile along the path marked on the lower STM image, with two triangles marking the portion of the scan corresponding to the segment on the lower image. The surface roughness appears to be approximately 250 nm, with some peaks (light regions in the lower image) measuring 750 nm.

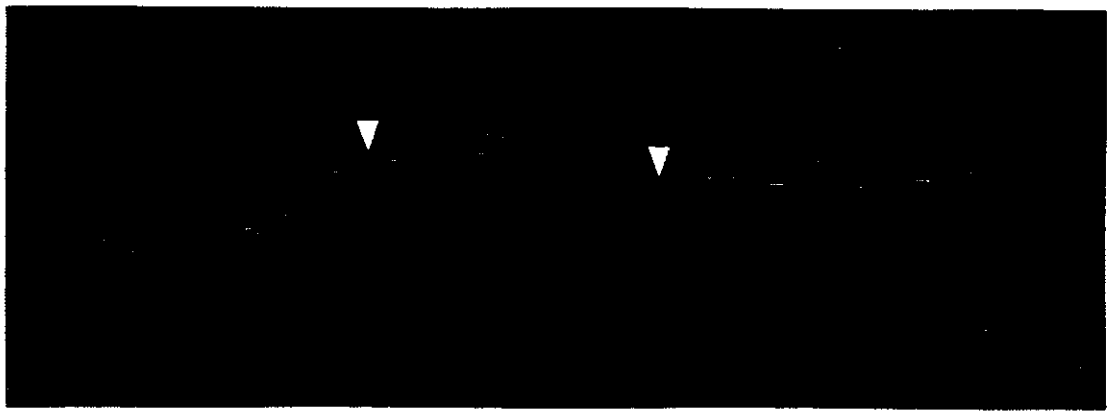

MT-001

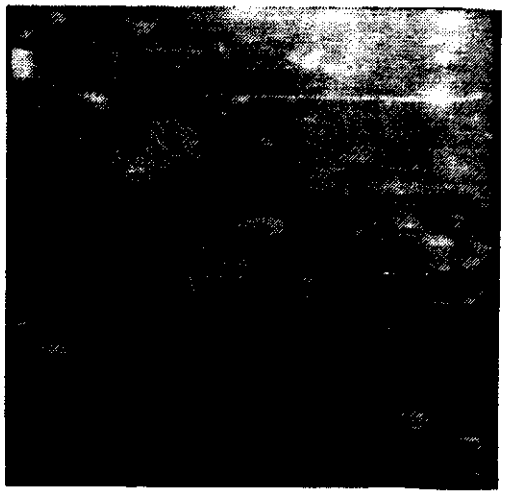

Figure A5. **(Lower)**: STM images of type MTL alumina-filled PPMI film (thickness: 25 μm) with a 30 nm gold deposition layer.
(Upper): The surface roughness profile along the path marked on the lower STM image, with two triangles marking the portion of the scan corresponding to the segment on the lower image. The surface roughness appears to be approximately 250 nm.

REFERENCES

1. K.W. Garrett and H.M. Rosenberg, "The Thermal Conductivity of Epoxy-Resin/Powder Composite Materials", J. Phys. D: Appl. Phys. 7, 1247-1258 (1974).

2. C. Schmidt, "Influence of the Kapitza Resistance on the Thermal Conductivity of Filled Epoxies", Cryogen. 15/1, 17-20 (1975).

3. F.F.T. de Araujo and H.M. Rosenberg, "The Thermal Conductivity of Epoxy-Resin/Metal-Powder Composite Materials from 1.7 to 300 K", J. Phys. D: Appl. Phys. 9, 665-675 (1976).

4. R.E. Meredith and C.W. Tobias, "Resistance to Potential Flow through a Cubical Array of Spheres", J. Appl. Phys. 31/7, 1270-3 (1960).

5. Rayleigh, Lord, "On the Influence of Obstacles Arranged in Rectangular Order Upon the Properties of a Medium", Phil. Mag. 34, 481-502 (1892).

6. R. Radebaugh, N.V. Frederick and J.D. Siegwarth, "Flexible Laminates for Thermally Grounded Terminal Strips and Shielded Electrical Leads at Low Temperatures", Cryogen. 13/1, 41-43 (Jan 1973).

7. M. Locatelli, D. Arnaud and M. Routin, "Thermal Conductivity of Some Insulating Materials Below 1 K", Cryogen. 16/6, 374-375 (1976).

8. G. Claudet, F. Disdier and M. Locatelli, "Interesting Low-Temperature Thermal and Mechanical Properties of a Particular Powder-Filled Polyimide", pp. 131-140 in Nonmetallic Materials and Composites at Low Temperatures, Ed. by A.F. Clark, R.P. Reed and G. Hartwig (Plenum, N.Y., 1979).

9. D. Howling, E. Mendoza and J. Zimmerman, "Preliminary Experiments on the Temperature-wave Method of Measuring Specific Heats of Metals at Low Temperatures", Proc. R. Soc. London, Ser. A. 229, 86-109 (1955).

10. M. Van de Voorde, "Temperature Irradiation Effects on Materials and Components for Superconducting Magnets for High Energy Physics Applications", CERN 77-03 ISR Division (July 1977).

11. A.G. Muller, "Properties of Plastic Tapes for Cryogenic Power Cable Insulation", pp. 339-363 in Nonmetallic Materials and Composites at Low Temperatures, ed. by A.F. Clark, R.P. Reed and G. Hartwig (Plenum, N.Y., 1979).

12. Stefan L. Wipf. "Low-Temperature Heat Transfer by Contact in Vacuo, and Thermal Conductivity of Kapton", Proc. of the 9th Int. Conf. on Magnet Technology, C. Marinucci and P. Weymuth, Eds., pp. 692-695 (Swiss Inst. Nucl. Res., Villigen, 1985).

13. C.L. Choy, W.P. Leung and Y.K. Ng. "Thermal Diffusivity of Polymer Films by the Flash Radiometry Method", J. Polym. Sci.: Part B: Polym. Phys. 25, 1779-1799 (1987).

14. A. Witek, O. Guerrero and David G. Onn. "Comparison of Two Techniques for Thermal Transport Studies in Polymer-Based Thick Films", to be published, 1990.

15. David K. Lambert, "Polyimide Film on Silicon: Use of IR Emission Modulation to Obtain Thermal Conductivity", to be published (1989).

16. R.C. Steere, "Thermal Properties of Thin-Film Polymers by Transient Heating", J. Appl. Phys. 37/9, 3338-3344 (1966).

17. J.G. Hust and R. Boscardin. "Thermal Conductivity of Polyester-amide-imide Film", Cryogen. 21/5, 297-298 (1981).

18. Hoosung Lee. "Rapid Measurement of Thermal Conductivity of Polymer Films", Rev. Sci. Instrum. 53/6, 884-887 (1982).

19. J.G. Hust and J. Arvidson. "Thermal Conductivity of Glass Fiber/Epoxy Composite Support Bands for Cryogenic Dewars", National Institute of Standards and Technology (U.S.), Internal Report No. 275.03-78-2, (1978).

20. J.G. Hust and A.B. Lankford. "Comments on the Measurement of Thermal Conductivity and Presentation of a Thermal Conductivity Integral Method", Int. J. Thermophys. 3/1, 67-77 (1982).